PARAMETRIC STUDY OF REFORMING OF GLYCEROL TO HYDROGEN OVER PRECIOUS METAL CATALYSTS IN A MICROCHANNEL REACTOR

by

Can Ekici

B.S., Chemical Engineering, Boğaziçi University, 2012

Submitted to the Institute for Graduate Studies in
Science and Engineering in partial fulfillment of
the requirements for the degree of
Master of Science

Graduate Program in Chemical Engineering
Boğaziçi University

2014

PARAMETRIC STUDY OF REFORMING OF GLYCEROL TO HYDROGEN OVER PRECIOUS METAL CATALYSTS IN A MICROCHANNEL REACTOR

APPROVED BY:

Assoc. Prof. Ahmet Kerim Avcı ...…….
(Thesis Supervisor)

Asst. Prof. Alper Uzun ...…….

Prof. Ramazan Yıldırım …….

DATE OF APPROVAL: 15.10.2014

to my family

ACKNOWLEDGEMENTS

I would like to express my gratitude to my supervisor Assoc. Prof. Ahmet Kerim Avcı, whose guidance and wise advices enlightened my way during my MS thesis. Writing this thesis would not have been possible without his guidance and encouragement. It was a pleasure and a privilege to work with him.

I would like to acknowledge my thesis committee, Prof. Ramazan Yıldırım and Asst. Prof. Alper Uzun for devoting their valuable time to read and comment on my thesis.

My special thanks go to H. Onur Kavaklı for his guidance during my thesis work. He has been a great mentor to me. I am also very happy to have Sinan Koç as co-worker. His share in this work cannot be underestimated.

I want to thank Bilgi Dedeoğlu for his contribution to my reaction system. Melike Gürbüz, Başak Ünen, Yakup Bal and Murat Düzgünoğlu were also by my side whenever I needed. Thanks to Bilge Gedik Uluocak for her help in SEM and EDX analyses conducted at Boğaziçi University Research and Development Center.

I would like to thank Dilruba İnam, who has always been with me. Together we have lived the most beautiful years of our lives and she was still there in my lab with me waiting for my experiments to come to an end on many sunday afternoons. Her patience, support and love made everything a lot easier.

I would like to thank my friends Özgür Yaşar Çağlar, Serhat Erşahin, Mustafa Türkekul and Melis Yıldırım for their friendship and endless support. I was very lucky to have you by my side. Onur Önel, my best friend, wish you were here… Thank you for your support overseas. I always knew you were with me.

I would also like to thank İrem Şen, Cihan Kaya, Zeynep Erge Akbaş, Begüm Alaybeyoğlu, Emre Demirel, Doğa Demirhan, Barış Burnak, Kerem Aksakal, Utku Deniz,

Elif Erdinç and Burcu Karagöz and all my friends. Special thanks to all CATREL team members.

I devote this thesis to my family. This thesis would not have been possible without their love and encouragement. I am very lucky to have them.

Finally, financial supports provided by TÜBİTAK 1003 – Project No: 113M962 and TÜBİTAK 2211 are acknowledged.

ABSTRACT

PARAMETRIC STUDY OF REFORMING OF GLYCEROL TO HYDROGEN OVER PRECIOUS METAL CATALYSTS IN A MICROCHANNEL REACTOR

The purpose of this study is to construct a system to conduct glycerol steam reforming experiments in a microchannel reactor and to investigate how different parameters (temperature, steam-to-carbon ratio, total flow rate and reactant composition) affect the glycerol conversion and selectivities of gaseous products. Three precious metal catalysts (2 wt.% Rh/Al_2O_3, 2 wt.% Pt/Al_2O_3 and 2 wt.% Ru/Al_2O_3) are prepared using incipient-to-wetness impregnation technique. Glycerol and water mixture is sprayed into the furnace with the help of inert gas, N_2. The condensables are collected in cold traps and the gaseous products are analyzed by two gas chromatographs. It is observed that glycerol conversion increases with temperature over all three catalysts. Rh turns out to be the best catalyst in terms of glycerol conversion. Temperature is determined as the key parameter to glycerol steam reforming. Pt/Al_2O_3 at 475 °C and Rh/Al_2O_3 at 500 °C give maximum H_2 selectivities. At high temperatures, H_2 selectivities decrease; CH_4, C_2H_4 and C_2H_6 selectivities increase. Temperature is determined as the key parameter to glycerol steam reforming. Steam-to-carbon ratio affects the products distribution via water gas shift. Higher steam-to-carbon ratios lead to higher H_2 selectivities. Increasing total flow rate negatively affects glycerol conversion, but no significant changes are observed on gaseous product selectivities. Increasing the reactant composition in the system leads to a decrease in both glycerol conversion and H_2 selectivity. Coke formation is inevitable in glycerol steam reforming. Over all three precious metal catalysts, even in blank tests, coke formation is observed. Amount of coke deposited is less on Rh-based catalysts. According to EDX results, targeted metal loading (2 wt.% Rh) is achieved in Rh catalyst. Spent Rh catalysts exhibit carbon formation, more carbon is deposited on entry region than exit region.

ÖZET

GLİSEROL BUHAR REFORMLANMASI İLE HİDROJEN ÜRETİMİNİN ASİL-METAL KATALİZÖRLÜ MİKROKANAL REAKTÖR DÜZENLERİNDE İNCELENMESİ

Bu çalışmada, gliserol buhar reformlamasını mikrokanal reaktör düzeninde gerçekleştirmek amacıyla bir düzenek oluşturulmuş ve sıcaklık, besleme akımındaki molar buhar-karbon oranı, toplam akış hızı ve tepkimeye giren maddelerin reaktör içindeki oranı gibi değişkenlerin gliseröl dönüşümünü ve ürün seçiciliklerini nasıl etkilediği incelenmiştir. Üç farklı asil-metal katalizör (ağırlıkça 2% Rh/Al_2O_3, 2 % Pt/Al_2O_3 ve 2 % Ru/Al_2O_3) ardışık emdirme tekniği kullanılarak hazırlanmış ve mikrokanal konfigürasyonunu elde etmek için metal plakaya kaplanmıştır. Gliserol ve su karışımı denge gazı (N_2) yardımıyla fırının içine püskürtülmüştür. Sıvı maddeler soğuk tuzaklarda toplanmıştır ve gaz haldeki ürünler iki adet gaz kromatografiyla analiz edilmiştir. Sıcaklıkla gliserol dönüşümünün artması tüm katalizörler üzerinde gözlenmiştir. Rh katalizörün gliserol dönüşümünde en iyi katalizör olduğu belirlenmiştir (24% dönüşüm, 600 °C, buhar/karbon=5). Pt/Al_2O_3 475 °C'de ve Rh/Al_2O_3 500 °C'de, buhar-karbon oranı 5 iken, en fazla hidrojen seçiciliği vermektedir (sırasıyla 10.1 ve 9.6 mol H_2 / mol dönüşüme uğrayan gliserol). Yüksek sıcaklıklarda, H_2 seçiciliği azalmıştır ve CH_4, C_2H_4 and C_2H_6 seçicilikleri artmıştır. Besleme akımındaki molar buhar-karbon oranındaki değişim ürün dağılımını su-gazı değişimi reaksiyonu üzerinden değiştirmektedir. Yüksek buhar-karbon oranı H_2 seçiciliğini arttırmıştır. Toplam akış hızını arttırmak gliserol dönüşümünü olumsuz etkilemiştir; ancak gaz ürünlerin dağılımında değişiklik gözlenmemiştir. Reaksiyona girenlerin reaktör içindeki oranını arttırmak, yani besleme akımındaki denge gazını azaltmak hem gliserol dönüşümünü hem de H_2 seçiciliğini azaltmıştır. Tüm deneylerde karbon oluşumu gözlenmiştir. Oluşan karbon miktarının Rh katalizörde daha az olduğu belirlenmiştir. EDX sonuçlarına göre, katalizörde hedeflenen Rh yüzdesine (ağırlıkça 2% Rh) ulaşılmıştır. Reaksiyona girmiş Rh katalizörün çıkış kısmına kıyasla giriş kısmında daha fazla karbon birikimi olmuştur.

TABLE OF CONTENTS

ACKNOWLEDGEMENTS iv
ABSTRACT vi
ÖZET vii
LIST OF FIGURES x
LIST OF TABLES xiii
LIST OF SYMBOLS xiv
LIST OF ACRONYMS/ABBREVIATIONS xv
1. INTRODUCTION 1
2. LITERATURE SURVEY 4
2.1. Microchannel Reactors 4
2.2. Glycerol Steam Reforming 5
2.3. Precious Metal Catalysts for Glycerol Steam Reforming 7
2.3.1. Rh Based Catalysts 7
2.3.2. Pt Based Catalysts 8
2.3.3. Ru Based Catalysts 10
2.4. Kinetic Expressions over Precious Metal Catalysts 11
2.5. Precious Metal Catalysts for Oxidative Steam Reforming 12
3. EXPERIMENTAL WORK 14
3.1. Materials 14
3.1.1. Chemicals 14
3.1.2. Gases and Liquids 14
3.2. Experimental Systems 15
3.2.1. Catalyst Preparation System 15
3.2.2. Catalyst Characterization System 16
3.2.3. Catalytic Reaction System 16
3.2.4. Product Analysis System 21
3.3. Catalyst Preparation and Pretreatment 24
3.3.1. Preparation of Support 24
3.3.2. Preparation of Active Catalysts 25
3.3.3. Catalyst Coating on Microchannel Plates 26

3.3.4 Pretreatment 27
3.4. Reaction Tests 27
3.4.1. Blank Tests 27
3.4.2. Steam Reforming of Glycerol in Microchannel Reactor 28
4. RESULTS AND DISCUSSION 32
4.1. Effect of Temperature 32
4.2. Effect of Steam-to-Carbon Ratio 40
4.3. Effect of Total Flow Rate 47
4.4. Effect of Reactant Composition 49
4.5 Catalyst Characterization 51
5. CONCLUSIONS AND RECOMMENDATIONS 54
5.1. Conclusions 54
5.2. Recommendations 55
APPENDIX A: CALIBRATION OF MASS FLOW CONTROLLERS 56
APPENDIX B: CALIBRATION OF THE GAS CHROMATOGRAPHS 57
REFERENCES 61

LIST OF FIGURES

Figure 3.1.	The Impregnation System. ……...	16
Figure 3.2.	Feed Section of Glycerol Steam Reforming System. ……...	17
Figure 3.3.	Different Configurations to Introduce Liquid Reactant Mixture into Furnace. ……	18
Figure 3.4.	Reaction Section of Glycerol Steam Reforming System. ……	19
Figure 3.5.	Post-reaction Section of Glycerol Steam Reforming System. …….	20
Figure 3.6.	Gas Chromatographs Used in Glycerol Steam Reforming System. …	21
Figure 3.7.	Schematic Diagram of the Reaction System. ……...	23
Figure 3.8.	Microreactor Configuration a. Coated Microchannel Reactor b. Location of Steel Housing in Quartz Tube. …….	27
Figure 4.1.	Glycerol Conversion vs Temperature (S/C=5, N_2 flow: 48 NmL min^{-1}, Total flow: 96 NmL min^{-1}). …….	33
Figure 4.2.	H_2 Selectivity vs Temperature (S/C=5, N_2 flow: 48 NmL min^{-1}, Total flow: 96 NmL min-1). ……..	34
Figure 4.3.	CO_2 Selectivity vs Temperature (S/C=5, N_2 flow: 48 NmL min^{-1}, Total flow: 96 NmL min^{-1}). ……..	35
Figure 4.4.	CO Selectivity vs Temperature (S/C=5, N_2 flow: 48 NmL min^{-1}, Total flow: 96 NmL min^{-1}). ..…….....	36

Figure 4.5. CH_4 Selectivity vs Temperature (S/C=5, N_2 flow: 48 NmL min^{-1}, Total flow: 96 NmL min^{-1}). …….. 37

Figure 4.6. C_2H_4 Selectivity vs Temperature (S/C=5, N_2 flow: 48 NmL min^{-1}, Total flow: 96 NmL min^{-1}). …….. 38

Figure 4.7. C_2H_6 Selectivity vs Temperature (S/C=5, N_2 flow: 48 NmL min^{-1}, Total flow: 96 NmL min^{-1}). ……..... 39

Figure 4.8. Glycerol Conversion vs Steam-to-Carbon Ratio. ……. 40

Figure 4.9. H_2 Selectivity vs Steam-to-Carbon Ratio. …… 41

Figure 4.10. CO Selectivity vs Steam-to-Carbon Ratio. …….. 42

Figure 4.11. CO_2 Selectivity vs Steam-to-Carbon Ratio. ……. 44

Figure 4.12. CH_4 Selectivity vs Steam-to-Carbon Ratio. ……. 44

Figure 4.13. C_2H_4 Selectivity vs Steam-to-Carbon Ratio. …… 45

Figure 4.14. C_2H_6 Selectivity vs Steam-to-Carbon Ratio. ……..... 46

Figure 4.15. Glycerol Conversion and H_2 Selectivity vs Total Flow Rate. …….. 47

Figure 4.16. Selectivities of Gaseous Products vs Total Flow Rate. …… 48

Figure 4.17. Glycerol Conversion and H_2 Selectivity vs Reactant Composition. … 49

Figure 4.18. Selectivities of Gaseous Products vs Reactant Composition. …….. 50

Figure 4.19. Catalyst-Coated Microchannel Plates a. Typical Spent Rh Catalyst (600 °C, S/C=3) b. Reduced Rh Catalyst. …… 52

Figure 4.20. SEM Micro Images of Reduced and Spent Rh Catalysts. …… 53

Figure A.1. Calibration Curve of the N_2 Mass Flow Controller. …… 56

Figure A.2. Calibration Curve of the H_2 Mass Flow Controller. …… 56

Figure B.1. Calibration Curve for N_2. …… 57

Figure B.2. Calibration Curve for H_2. …… 57

Figure B.3. Calibration Curve for CH_4. …….. 58

Figure B.4. Calibration Curve for CO. …… 58

Figure B.5. Calibration Curve for CH_4. ……..... 59

Figure B.6. Calibration Curve for CO_2. ……..... 59

Figure B.7. Calibration Curve for C_2H_4. ……..…….. 60

Figure B.8. Calibration Curve for C_2H_6. ……..…….. 60

LIST OF TABLES

Table 3.1.	Chemicals used for catalyst synthesis.	14
Table 3.2.	Specifications and the applications of gases used.	15
Table 3.3.	GC conditions for product gas analysis. …….....	22
Table 3.4.	Alumina support preparation procedures. ……	24
Table 3.5.	List of blank tests in microchannel reactor.	28
Table 3.6.	List of experiments for parametric study of glycerol. ……..	30
Table 4.1.	Surface composition of a typical spent Rh catalyst.	52

LIST OF SYMBOLS

D	Diameter of the housing (mm)
L	Length of the plate (mm)
T	Temperature (°C)
W	Width of the microchannel (mm)
υ_i	Flow rate of the species i ($ml.min^{-1}$)
$X_{glycerol}$	Glycerol conversion

LIST OF ACRONYMS/ABBREVIATIONS

BET	Brunauer-Emmett-Teller
BSE	Backscattering Electron
EDX	Energy Dispersive X-ray Analysis
GC	Gas Chromatography
HPLC	High Pressure Liquid Chromatography
ID	Inside Diameter
PID	Proportional Integral Derivative
S/C	Steam-to-Carbon Ratio
SEM	Scanning Electron Microscopy
SR	Steam Reforming
TCD	Thermal Conductivity Detector
W/F	Catalyst Weight to Feed Flow Rate Ratio

1. INTRODUCTION

The facts associated with global depletion of oil reserves and the environmental issues such as global warming led people to search for alternative energy sources other than crude oil. Among several alternatives, biodiesel, a renewable fuel that can be obtained by transesterification of animal or vegetable oils with methyl or ethyl alcohol, has recently received interest as a sustainable and clean energy source. Biodiesel has many similarities with its petroleum-based counterpart; when blended with petroleum diesel it can be transported with existing infrastructure and used directly in existing diesel vehicles. However, the current price of biodiesel is higher than that of petroleum diesel. In order to increase widespread use of biodiesel, its price should be lowered (Avasthi *et al*., 2013).

Glycerol is the simplest trihydric alcohol and it is a versatile chemical with numerous applications in food, cosmetics and pharmaceuticals (Christoph *et al*., 2000). Glycerol is usually classified as natural or synthetic. Natural glycerol can be produced by the high-pressure splitting of water and fat, by the transesterification process as a byproduct in biodiesel synthesis, or by saponification in soap manufacturing. Synthetic glycerol is derived from propylene oxidation and chlorination. Natural glycerol, particularly the one produced by saponification, has accounted for most of the market supply in the last few decades. However, because of the recent boom in biodiesel production, glycerol produced as a byproduct of transesterification is gradually surpassing production of all other compositions. As the glycerol production tends to grow drastically, approximately 3 megatons of crude glycerol is expected to be produced by 2020, whereas the annual commercial need will be less than 500 kilotons (Lin, 2013). Purification of crude glycerol from the biodiesel plants, as well as the disposal of excess glycerol is challenging and expensive (Avasthi *et al*., 2013). For every 9 kg of biodiesel produced, 1 kg glycerol is produced as by-product. One way of using excess glycerol produced is to convert it to hydrogen or synthesis gas via the steam reforming process. Hydrogen is a clean energy source and it has great importance in ammonia production, petroleum processing and power generation in fuel cells (Avasthi *et al*., 2013). Synthesis gas is used as a feedstock for the production of hydrocarbons by Fischer-Tropsch synthesis and of methanol.

Methanol is also one of the reactants in biodiesel production, so glycerol may indirectly supply feedstock for biodiesel production (Lin, 2013).

Steam reforming of glycerol (Reaction 1.1) is the most general method to convert glycerol to hydrogen and/or synthesis gas. This method is a combination of pyrolysis of glycerol and water-gas shift reactions (Lin, 2013). In addition to these two major reactions, other side reactions such as coke formation and methanation take place (Slinn *et al*., 2008). Steam reforming of glycerol occurs mostly in the gas phase, so heating is required to vaporize the reactants:

$$C_3H_8O_3 + xH_2O \leftrightarrow (3\text{-}x)CO + xCO_2 + (4+x)H_2 \qquad (1.1)$$

Nickel based catalysts are the most commonly used catalysts for steam reforming. Alternatively, precious metal catalysts are also used in steam reforming of glycerol. In general, Ni, Co, Pt, Rh and Ru are the most common active metals and alumina, ceria, zirconia are the favorite supports (Lin, 2013). Even though many combinations of the aforementioned metals and supports are studied, the reactor type is limited to packed-bed type and the impact of reactor configuration on glycerol steam reforming is not investigated in the literature. It is recently shown that catalytic microchannel reactors allow better utilization of the catalyst by enhanced heat transfer properties and lead to higher reactant conversions (Karakaya *et al*., 2012). Investigation of the potential advantages of microchannel reactor configuration in precious metal catalyzed glycerol reforming is the focal point of this study.

In this work, an experimental set-up is designed and constructed to conduct glycerol steam reforming experiments in a catalytic microchannel reactor. The studies are carried out in the context of a parametric plan. The effects of temperature, feed composition, contact time and reactor configuration are investigated over various precious metal catalysts. In addition the structural changes on catalyst surface after reaction are examined by scanning electron microscopy (SEM) analysis.

This study contains five chapters. In Chapter 2, a literature survey is given about the experimental studies of steam reforming of glycerol over nickel based and precious metal

catalysts and oxidative steam reforming of glycerol. In Chapter 3, experimental set-up is explained in detail. Techniques and procedures followed for catalyst preparation and catalytic activity tests are also included. Chapter 4 consists of the results and discussions obtained from the catalytic activity tests and parametric study. In Chapter 5 the conclusions drawn from this study and recommendations for future studies are stated.

2. LITERATURE SURVEY

2.1. Microchannel Reactors

At present, most of the industrial reactions are performed using techniques and apparatus that have been used for decades. Packed bed reactors are preferred for many reactions in industry. Although there are numerous studies about the nature of packed bed reactors, it is still a challenge to scale up studied laboratory reactions for mass production. In addition to that, heat and mass transfer limitations and large reactor volumes remain as the drawbacks of the packed bed reactors. Microchannel reactors, that are described below, have the potential to overcome some of the disadvantages of the packed bed reactors.

Microchannel reactors consist of parallel, identical channels with diameters between 10 to several hundred micrometers. This provides surface areas in the range of ca. 10000 – 50000 m^2/m^3 and volume reductions up to ca. 90% (Ehrfeld *et al*., 2001; Lerou *et al*., 2010). In addition to the fact that the transition from laboratory scale to industrial scale operation is much easier in microchannel reactors, the compact and solid nature of the microchannel reactors enhance heat transfer, which is very important especially for rapid exothermic reactions. High surface area and high heat transfer coefficients prevent hot spot formations, which may harm the catalyst or change the product distribution (Hessel and Kolb, 2004; Kiwi-Minsker and Renken, 2005). Not only heat transfer, but also the mass transfer is enhanced in microchannel reactors. Since laminar flow is fully developed in microchannels, the Sherwood number, which is mass transfer coefficient multiplied by hydraulic diameter divided by the diffusion coefficient, reaches a constant value. This implies that as the hydraulic diameter gets smaller; the mass transfer coefficient gets larger, decreasing the mass transfer limitation (Fichtner *et al*., 2001). As the amount of gas or liquid in a single channel is limited, safer operating conditions are achieved for the reactions, such as partial oxidations, for runaway and explosion (Veser and Frauhammer, 2006). Also, the residence time distribution in microchannel reactors is very narrow because of the laminar flow regime in the channel, and this is advantageous when contact

times are important on product distribution, especially when trying to maximize a mid-product selectively (Hasebe, 2004).

To date, micro structured reactors have been fabricated from a variety of substrates including silicon, quartz, metals, polymers, ceramics and glass, with the choice of substrate being largely governed by the end use of the reactor and the fabrication technique employed. Consequently, when 'designing' a micro reactor, the substrate must be evaluated for chemical compatibility, thermal and pressure resistances and ease of fabrication. Depending on the substrate selected and the degree of complexity required, a suitable micro fabrication technique must be applied (Watts and Wiles, 2006).

In the literature, there is no gas phase glycerol steam reforming run in a microchannel reactor configuration. However, in methane steam reforming, it is recently shown that catalytic microchannel reactors allow better utilization of the catalyst by enhanced heat transfer properties and lead to higher reactant conversions (Karakaya *et al*., 2012). The advantages proven in methane steam reforming and the particular reactor geometry make microchannel reactors promising for gas phase glycerol steam reforming reaction.

2.2. Glycerol Steam Reforming

Steam reforming is a well-studied two step reaction and it is the most commonly used method to produce hydrogen and synthesis gas (Chiodo *et al*., 2010). Synthesis gas (syngas), a mixture of H_2 and CO, is an important feed stock for industrial processes such as Fischer-Tropsch synthesis and methanol production. The initiation of steam reforming of glycerol involves its decomposition into CO and H_2, via the pyrolysis reaction:

$$C_3H_8O_3 \leftrightarrow 3CO + 4H_2 \tag{2.1}$$

CO produced in glycerol pyrolysis reacts with steam, which is the water gas shift reaction:

$$CO + H_2O \leftrightarrow CO_2 + H_2 \quad (2.2)$$

Combination of Reactions 2.1 and 2.2, gives the overall glycerol steam reforming reaction:

$$C_3H_8O_3 + xH_2O \leftrightarrow (3\text{-}x)CO + xCO_2 + (4+x)H_2 \quad (1.1)$$

Here, 'x' indicates the degree of the water gas shift reaction involved, which ranges from 0 to 3. Based on the stoichiometry, the reaction shifts to glycerol pyrolysis when x = 0. Glycerol reforming to H_2 dominates at x = 3. Synthesis gas can be produced when x is between 0 and 3 (Lin, 2013). It is worth noting that, glycerol steam reforming is not the only reaction mechanism when glycerol and water come into contact at high temperatures. A list of possible side reactions are as follows (Slinn *et al.,* 2008):

$$C + H_2O \leftrightarrow CO + H_2 \quad (2.3)$$

$$C + 2H_2 \leftrightarrow CH_4 \quad (2.4)$$

$$CO + 3H_2 \leftrightarrow CH_4 + H_2O \quad (2.5)$$

$$CO_2 + 4H_2 \leftrightarrow CH_4 + 2H_2O \quad (2.6)$$

$$C + CO_2 \leftrightarrow 2CO \quad (2.7)$$

At high temperatures, glycerol may decompose into non equilibrium products, most commonly through dehydration and dehydrogenation routes. Dehydration produces hydroxyacetone and 3-hydroxypropanal, the latter being the precursor of acrolein (Lin, 2013):

$$C_3H_8O_3 \leftrightarrow C_3H_6O_2 + H_2O \quad (2.8)$$

$$C_3H_6O_2 \leftrightarrow C_3H_4O + H_2O \quad (2.9)$$

Dehydrogenation generates glyceraldehydes and dihydroxyacetone (Lin, 2013):

$$C_3H_8O_3 \leftrightarrow C_3H_6O_3 + H_2 \quad (2.10)$$

Oxidative steam reforming of glycerol, which is summarized below (Equation 2.11), is a developing research field. Due to the exothermic nature of the reactions in this mechanism, the reactions have fast start-ups. With proper insulation, the reactor design can be made without an external heat source. Carbon deposition, which is commonly seen in steam reforming, is negligible with the oxidative reactions. This feature extends the catalyst life and ensures long-time operation (Lin, 2013):

$$C_3H_8O_3 + \frac{3}{4}O_2 + \frac{3}{2}H_2O \rightarrow 3CO_2 + \frac{11}{2}H_2 \qquad (2.11)$$

2.3. Precious Metal Catalysts for Glycerol Steam Reforming

Steam reforming is a process that is commonly used in petroleum refineries to convert natural gas and naphthas into synthesis gas. The process involves the use of nickel-based catalysts. It is likely that glycerol steam reforming can also be performed in oil refineries, therefore, nickel-based catalysts are frequently used in glycerol steam reforming studies. Alternatively, precious metal catalysts are also used in steam reforming of glycerol. In general, Ni, Co, Pt, Rh and Ru are the most common active metals and alumina, ceria, zirconia are the favorite supports (Lin, 2013).

2.3.1 Rh Based Catalysts

Rh based catalysts are proven to be effective in the production of synthesis gas by ethanol steam reforming. On the basis of this experience, Chiodo and co-workers (2010) evaluated the behavior of rhodium based catalysts in glycerol steam reforming. Before experimenting the reaction with catalyst, knowing that glycerol is not a thermally stable molecule, a preliminary test without catalyst was carried out at 1073 K and S/C=3. After a 4-hour experiment, 65% glycerol conversion is achieved with the selectivities of 50% to CO, 25% to olefins (mostly C_2H_4), 13% to CH_4, 10% to H_2 and 1% to CO_2 (Chiodo *et al.*, 2010).

The stability of 5 wt.% Rh/Al_2O_3 was tested in terms of H_2 selectivity. The test was conducted at 1073 K with S/C=3 and a total flow of 130 NmL min^{-1}. H_2 selectivity (mol H_2

/ mol glycerol converted) dropped from 3.5 to 1.0 after a 20 hour operation, with a sharp decrease (down to 1.5) in the first 6 hours. A residual H_2 production was observed, due to thermal decomposition of glycerol (Chiodo *et al.*, 2010). The effect of temperature on H_2 selectivity was investigated by repeating the experiment at 723 K, 823 K and 923 K. In the experiments conducted at 723 K and 1073 K, H_2 selectivity decreases to 1.0 after 20 hours. However, at 823 K and 923 K, H_2 selectivity decreased to about 3.0 from 4.0 and 5.0, respectively. Thermodynamic analysis was made to explain the findings and it was found that, thermodynamically, H_2 selectivity reaches a maximum at 923 K, and then decreases slightly. The experiment at 1073 K pointed out a sharp decrease in H_2 selectivity after 923 K, which was not foreseen in thermodynamic analysis. TEM analysis on spent samples highlighted a substantial morphological difference between catalysts used at different temperatures. In terms of metal sintering it was observed that up to 923 K, the particle size distributions of Rh remain unchanged, while larger Rh particles were observed on the sample at 1073 K, which is a sign of sintering at that temperature. As regard of coke formation, up to 923 K, filamentous type of coke formation was observed while at 1073 K, encapsulating carbon formation was detected. Sintering and encapsulating carbon formation were held responsible for the sudden decrease in H_2 selectivity after 923 K, in contrast with the thermodynamic analysis (Chiodo *et al*., 2010).

Gas phase glycerol conversion and H_2 selectivity data were collected during a 100-hour time-on-stream experiment. At 923 K and S/C=3, glycerol conversion decreased from 90% to 45% and H_2 selectivity decreased from 5.0 to 2.5. These findings were stated to be clear evidances of coke formation that deactivated the Rh catalyst (Chiodo *et al*., 2010).

2.3.2 Pt Based Catalysts

In their work, Dumesic and co-workers (2010) investigated the effect of Pt loaded catalysts on glycerol steam reforming at different temperatures, glycerol feed concentrations and contact times. Pt catalysts on five different support materials were prepared and tested for stability for 50 hours at 623 K with a feed solution of 30wt.% glycerol in water. 1.0 gram of 5 wt.% Pt on Al_2O_3, ZrO_2, CeO_2/ZrO_2 and MgO/ZrO_2 and 60 mg of 5 wt.% Pt/C catalysts were used in the stability test. Among them, Pt/C showed stable conversion of glycerol at about 65%. Pt/Al_2O_3 showed glycerol conversion higher

than 95%, followed by a rapid deactivation after 30 hours of operation. Deactivation was observed in the experiments conducted with other catalysts, $Pt/MgO/ZrO_2$ catalyst was found to be the least stable one among all (Dumesic *et al*., 2010).

Slinn and co-workers (2008) studied steam reforming of pure and crude glycerol over Pt/Al_2O_3 catalyst and compared them with each other. Experiments involving pure glycerol showed that steam reforming dominates carbon formation at temperatures above 700 °C, at flow rates 0.6 mol glycerol/min.kgcat and at molar steam/carbon ratios over 0.5. Optimum reformer performance was reached at the temperature of 880 °C, flow rate of 0.12 mol glycerol/min.kgcat and steam/carbon ratio of 2.5. At flow rates above 0.20 mol/min.kgcat and at steam/carbon ratios less than 0.5, high carbon deposition was observed (Slinn *et al*., 2008). Under the same reaction conditions, crude glycerol gave 70% of the selectivity of pure glycerol. Because of the fatty impurities in the crude glycerol, the reforming was harder and carbon deposition was more significant (Slinn *et al*., 2008).

Glycerol steam reforming over Pt/Al_2O_3 and effect of addition of La_2O_3 and CeO_2 were investigated in detail by Fornasiero and co-workers (2010). The experiments were conducted at different temperatures, with 30 wt.% glycerol in aqueous solution feed rate of 0.32 NmL min^{-1}. Among 1.0 gram of 3 wt.% Pt/Al_2O_3, 3 wt.% $Pt/La_2O_3/Al_2O_3$ and 3 wt.% $Pt/CeO_2/Al_2O_3$ samples, Pt/Al_2O_3 exhibited a poor activity towards glycerol steam reforming at low temperatures between 350-400 °C. The effluent gas stream was rich in hydrocarbons (CH_4, C_2H_4 and C_2H_6). Various liquid by-products such as hydroxyacetone, 1,2-propanediol, ethylene glycol and their monoesthers with acetic acid, acrolein and acrylic acid, were detected in trace amounts. The poor activity of Pt/Al_2O_3 catalyst towards glycerol steam reforming was explained to be the result of a complex network of side reactions, including dehydration, condensation and polymerization reactions, promoted by the acid sites of the support as well as dehydrogenation and hydrogenation reactions promoted by the Pt nanoparticles (Fornasiero *et al*., 2010). Pt/Al_2O_3 catalysts doped with La_2O_3 and CeO_2 showed similar trends with Pt/Al_2O_3 up to 300 °C, but a sharp increase was observed between 350-400 °C, leading to glycerol conversion close to 100%. At temperatures above 350 °C, significant increase in CO_2 and H_2 production was observed, which was an indication of the presence of water gas shift reaction. CH_4 was the only major by-product and only trace amounts of C_2H_4 and C_2H_6 were present. It was concluded

that Pt/Al_2O_3 catalyst promoted H_2 production only at temperatures higher than 500 °C, which resulted from the side reactions promoted by acidic sites on the alumina support. Greater amount of undesired by-products were detected in the effluent stream. La_2O_3 and CeO_2 deposition on Al_2O_3 improved the catalytic performance of Pt nanoparticles by decreasing the acidity of the support, achieving complete glycerol conversion at 350 °C. These additions promoted the water gas shift reaction. Also, addition of La_2O_3 and CeO_2 improved the catalyst stability. The amount of carbon deposited was significantly reduced compared to the plain Pt/Al_2O_3 catalyst. CeO_2-doped catalyst deactivated after 20 hours at 350 °C, while a higher stability was shown by the La_2O_3-doped catalyst that ran over 50 hours (Fornasiero *et al*., 2010).

Nichio and co-workers (2010) investigated Pt based catalysts loaded on various support, concentrating on the intermediate products during steam reforming reaction. It was concluded that supports with acidic properties (like Al_2O_3) promoted lateral reactions of dehydration, dehydrogenation, hydrogenolysis and condensation. Therefore, fast deactivation of catalysts by coke formation occured (Nichio *et al*., 2010).

2.3.3 Ru Based Catalysts

Suzuki and his co-workers (2005) studied group 8-10 elements as the active metals in glycerol steam reforming. The reactions were conducted over La_2O_3 catalysts at temperatures between 500–600 °C and at a steam/carbon ratio of 3.3. The order of the activity of the metals were found as Ru ≈ Rh > Ni > Ir > Co > Pt > Pd > Fe. Effect of different supports was investigated using 3 wt.% Ru as the active metal. Y_2O_3 and ZrO_2 supported catalysts showed high glycerol conversion and high H_2 selectivity. Ru/MgO showed very low glycerol conversion. Although Al_2O_3 was used as a favorable support for the steam reforming of hydrocarbons, Ru/Al_2O_3 exhibited the lowest conversion in the steam reforming of glycerol. Among the catalysts, 3 wt.% Ru on Y_2O_3 turned out to be the best performing catalyst, achieving more than 80% H_2 selectivity. The H_2 selectivity increased as the Ru loading increased up to 3%, and a further increase in Ru to 5 wt.% did not affect the results (Suzuki *et al*., 2005).

H_2 production from glycerol steam reforming over 5 wt.% Ru/Al_2O_3 catalyst in supercritical water was studied, where glycerol was brought into contact with water at high temperatures and pressures at a short reaction time. In this scenario, water served both as a dense solvent and a reactant. Experiments were conducted at temperatures between 700-800 °C and at 241 bar with feed ratios up to 40 wt.% glycerol, all at short reaction times varying from 1 second to 4 seconds. Over the temperature, residence times and water to glycerol mass ratio ranges analyzed, the conversion of glycerol always exceeded 99%. Glycerol was completely gasified to H_2, CO_2, CH_4 and small amounts of CO. H_2 selectivities were found to increase directly with temperature. CH_4 formed was reduced at low residence times. As glycerol weight percentage in the feed stream increased, H_2 selectivity decreased significantly and CH_4 formation increased (Gupta *et al.*, 2008).

Iulianelli and his co-workers (2011) investigated glycerol steam reforming to produce H_2 for proton exchange membrane fuel cells. The steam reforming reaction was performed using a dense palladium-silver membrane reactor in order to produce pure H_2 using 0.5 wt% Ru/Al_2O_3 as reforming catalyst. The set of experiments gave the best results of 57% glycerol conversion, 60% CO-free H_2 recovery under 400 °C and 5 bars, with steam-to-carbon ratio of 6.0. Carbon formation was observed as the main problem of the process (Iulianelli *et al.*, 2011).

2.4. Kinetic Expressions over Precious Metal Catalysts

There are two power law type kinetics proposed on glycerol steam reforming reaction over precious metal catalysts. Sutar and co-workers (2010) collected glycerol conversion versus space-time data using a fixed bed reactor over a commercial 5% Pt/C catalyst. After data analysis by the integral method, it was concluded that the reaction was first order with respect to glycerol. The reaction rate constant at 400 °C was found as $1.1x10^5$ $cm^3/(g_{cat}$ h). Additionally, it was established that the glycerol steam reforming reaction was favored when water was in excess quantities (e.g. when steam to glycerol ratio was 9) (Sutar et al., 2010). Another study on reaction kinetics of glycerol steam reforming was made using a fixed bed reactor over Ru/Al_2O_3 catalyst. Temperatures in the range of 350-500 °C and catalyst weight-to-glycerol inlet feed ratios of 0.4-1.98 g_{cat}.h/mol were studied. The increases in temperature, steam-to-glycerol ratio in feed and space time

caused the expected increase in H_2 selectivity. Using the integral method of analysis, the reaction order with respect to glycerol was determined as 1.0. The activation energy was found as 21.2 kJ/mol. Finally, it was found that first-order kinetics was valid at low glycerol partial pressures (Sundari and Vaidya, 2012).

2.5. Precious Metal Catalysts for Oxidative Steam Reforming

Oxidative steam reforming (OSR) of glycerol to H_2 is a topic that is studied less than steam reforming of glycerol. In general, oxidative steam reforming of glycerol studies is performed in micro packed reactors, between 600 and 1000 °C. Rh and Ni are the most studied active metals, whereas ceria and alumina are the favorite supports.

OSR of glycerol to H_2 gave very good glycerol conversions and satisfactory H_2 selectivities (Schmidt *et al.*, 2009). Autothermal steam reforming of glycerol (and of other volatile carbohydrates) over Rh and Pt based catalysts supported on alumina foams was tested at a contact time of approximately 10 ms (Schmidt *et al.*, 2006). They managed to achieve 99% glycerol conversion over Rh-Ce on gamma alumina catalyst with a H_2 selectivity of 79%. The optimum C/O_2 ratio was found to be 0.9 (Schmidt *et al.*, 2006). In another study, Schmidt and co-workers (2009) conducted catalytic partial oxidation of glycerol at temperatures above 600 °C and at contact times between 30-90 ms over Rh and Pt based catalysts. With the Rh catalyst, they reached maximum glycerol conversion of 90% and H_2 selectivity of 65% at a steam-to-carbon ratio of 0.66 (Schmidt *et al.*, 2009). The same group investigated the long time behavior of the catalytic partial oxidation of glycerol in an autothermal reactor over Rh catalyst supported on ceria-alumina. At the beginning of the experiment, the H_2 selectivity was at its maximum at 70%. The H_2 selectivity, however, declined as the experiment continued, and after a 450-hour continuous operation, the H_2 selectivity decreased down to 20%. This drastic change was caused by the catalyst deactivation (Schmidt *et al.*, 2010).

Lin and Liu studied the autothermal partial oxidation of glycerol over Pt, $LaMnO_3$, and $Pt/LaMnO_3$ coated monoliths. The optimization of the performance of $Pt/LaMnO_3$ was achieved at steam/carbon and C/O_2 ratios of 0.66 and 1.1, respectively, where glycerol

conversion reached 98%, yielded a H_2/CO ratio of 2.1, and produced the least hydrocarbon by-products with 6.1% (Lin and Liu, 2012).

3. EXPERIMENTAL WORK

3.1. Materials

3.1.1. Chemicals

All the chemicals used for catalyst preparation are presented in Table 3.1.

Table 3.1. Chemicals used in catalyst preparation.

Chemicals	**Specification**	**Source**	**Molecular weight**
Rhodium(III) nitrate	$Rh(NO_3)_3$ 10 wt.% Rh	Sigma-Aldrich	288.92
Tetraammineplatinum(II) nitrate	$[Pt(NH_3)_4]$ $(NO_3)_2$ 50.4wt%Pt	Sigma-Aldrich	387.22
Ruthenium(III) nitrosyl nitrate	$Ru(NO_3)_3(NO)$ 1.5 wt.%	Sigma-Aldrich	318.10
Gamma alumina (3 μm)	γ-Al_2O_3 80-120 m^2/g	Alfa-Aesar	101.96
FeCrAlY	FeCrAlY sheets	Goodfellow Cambridge	

3.1.2. Gases and Liquids

The gases N_2, H_2, Ar and He are used in experimental studies (Table 3.3) were supplied by Linde. The deionized water is obtained by Zeneer Water Purification System and its conductivity is less than 0.1 $\mu S.cm^{-1}$. Deionized water is used as a reactant in glycerol steam reforming. It is also used in catalyst synthesis, when preparing the catalyst and coating it onto micro plates. Glycerol with 99.5% purity is obtained from Sigma-Aldrich.

Table 3.2. Specifications and applications of the gases used.

Gas	Specification	Application
Argon	99.995% (Linde)	GC carrier gas
Helium	99.99% (Linde)	GC carrier gas
Nitrogen	99.99% (Linde)	GC calibration, inert
Carbon monoxide	99.999% (Linde)	GC calibration
Hydrogen	99.99% (Linde)	GC calibration, reducing agent
Carbon dioxide	99.99% (Linde)	GC calibration
Methane	99.70% (Linde)	GC calibration
Ethane	5%C_2H_6+95%N_2 (Linde)	GC calibration
Ethylene	5%C_2H_4+95%N_2 (Linde)	GC calibration

3.2. Experimental Systems

The experimental system used in this research mainly consists of four groups.

- Catalyst Preparation System: The setup used for preparing all the catalysts used in this study by incipient-to-wetness impregnation method.
- Catalyst Characterization System: Scanning Electron Microscopy (SEM) integrated with Energy Dispersive X-ray Spectroscopy (EDX) to analyze the structural properties of the catalysts.
- Catalytic Reaction System: The system used for catalytic activity tests, consisting of mass flow controllers for inlet gases, HPLC pump for water and glycerol mixture feed, reaction chamber controlled by three programmable temperature controllers and a microchannel reactor, together with two cold traps.
- Product Analysis System: Two online gas chromatographs are used for analyzing the composition of the product gases.

3.2.1. Catalyst Preparation System

Rh/Al_2O_3, Pt/Al_2O_3 and Ru/Al_2O_3 catalysts are prepared by incipient to wetness impregnation technique illustrated by Figure 3.1. The system consists of Retsch UR1

ultrasonic mixer which provides uniform mixing, a vacuum pump, a Buchner flask, silicone tubing and a Masterflex computerized-drive peristaltic pump which is used for impregnation of the solution to the support.

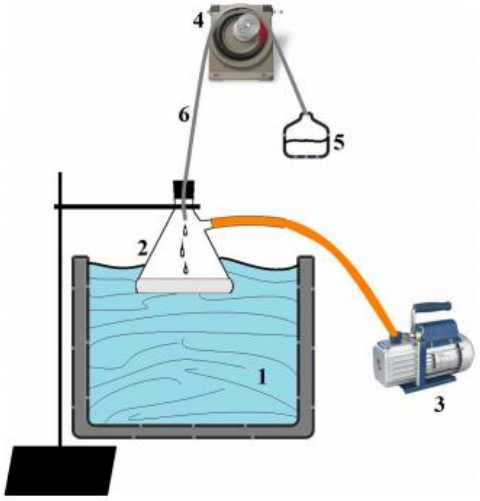

Figure 3.1. The Impregnation System: 1. Ultrasonic Mixer 2. Buchner Flask 3. Vacuum Pump 4. Peristaltic Pump 5.Aqueous Catalyst Solution 6. Silicon Tubing (Karakaya, 2012).

3.2.2. Catalyst Characterization System

The structural analyses of the catalyst samples were carried out at Boğaziçi University Advanced Technologies R&D Center through Backscattering Electron-Scanning Electron Microscopy (BSE-SEM) and Energy Dispersive X-ray Analyses (EDX) using a Philips XL30 ESEM-FEG system.

3.2.3. Catalytic Reaction System

The gas phase steam reforming of glycerol system was designed and constructed at Catalyst Technology and Reaction Engineering Laboratory (CATREL), Department of Chemical Engineering. The system is mainly composed of three sections (Figure 3.2):

- Feed section
- Reaction section
- Product analysis section.



Figure 3.2. Feed Section of Glycerol Steam Reforming System.

Feed preparation section is designed and constructed to carry reactant liquids (deionized water, glycerol), inert gas (N_2) and reducing agent (H_2) into the reaction section. Gaseous species (N_2, H_2), which are stored in the pressurized storage cylinders, are brought to mass flow controllers through gas regulators provided by Linde. Bronkhorst F-201CV series digital mass flow controllers are used to measure and control the flow rates of the gases. Calibrations of these mass flow controllers are made and the calibration curves are presented in Appendix A. Each gas is attached to the system through 1/8” stainless steel tubing separately so that flow of gases can be measured independently and desired feed compositions can be adjusted. Deionized water and glycerol mixture is fed to the system

using a Shimadzu LC-20AD HPLC pump with constant pulse-free flow. Liquid mixture travels towards the reaction section in a 1/16” stainless steel tube horizontally, until it meets the carrier gas, N_2, and it is directly sprayed into the 2.0 cm ID x 80 cm quartz reactor in the furnace.

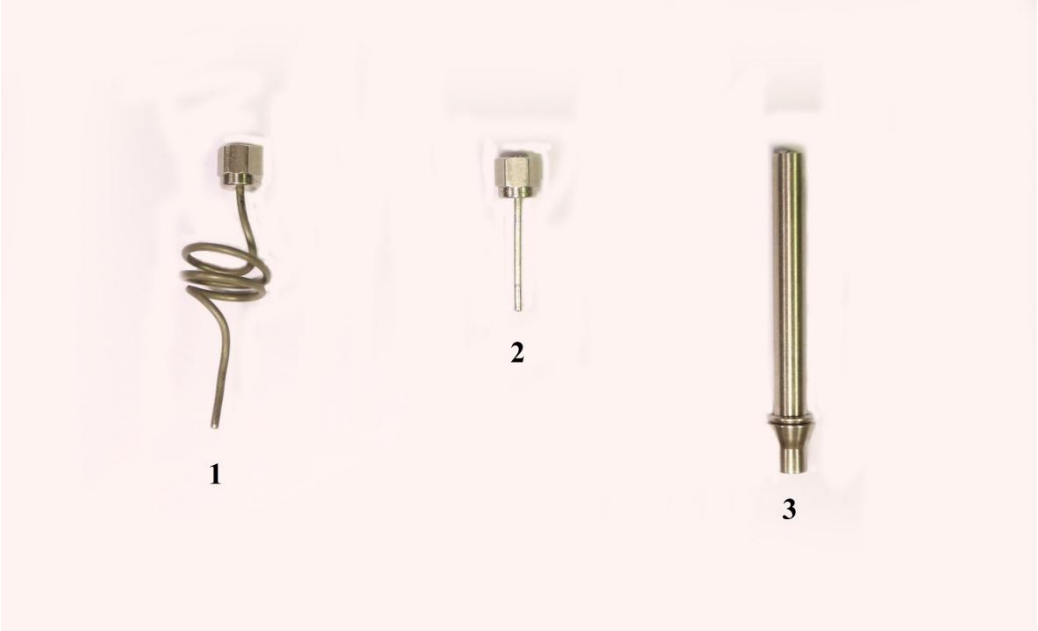

Figure 3.3. Different Configurations to Introduce Liquid Reactant Mixture into Furnace: 1. 1/16" Spiral-shaped. 2. 1/16" Straight. 3. 1/4" Straight.

Several different configurations were tried to enhance the glycerol-water mixing in the reactor entrance. Some of these configurations are shown in Figure 3.3. From the exit of the pump until the liquid reactant mixture is reached to the furnace, the tubings were heated up to 125 °C, so that it would help glycerol, which is a very viscous liquid, to move in the 1/16” pipe and to increase the temperature of the mixture, so the mixture would be vaporized more easily. But, high amount of coke was observed in the blank tests, probably because at 125 °C, water in the reactant mixture was vaporized and moved a lot faster than glycerol did, which reduced the steam-to-carbon ratio as glycerol reached the upper zone of the furnace, leading to coke formation. Without pre-heating the reactant mixture, it was fed into the system through a 1/4" pipe as seen in Figure 3.3. However, the liquid coming from the HPLC pump accumulated as droplets on the inner surface of the pipe and as they formed a droplet large enough, it fell into the reactor. A large droplet spent less time in the

upper zone of the furnace and complete vaporization and a good mixing were not guaranteed in this case. As the 1/4" pipe has a large inner diameter, an annular flow regime was achieved and no spraying effect was observed. Then, the liquid mixture was fed into the system through a 1/16" pipe without pre-heating. In that case, it was observed that N_2 was pushing the liquid down, through a much thinner pipe compared to 1/4", and spraying the liquid into the furnace. This configuration allowed liquid reactants to vaporize completely, as small liquid particles vaporize much faster, and a fast vaporization was key to good mixing. With that achieved, an improvement is made in the last configuration. A spiral-shaped 1/16" pipe, which is located in the upper zone of the furnace, is used to spray the liquid reactants (Figure 3.3). In the spiral configuration, however, more coke is observed, probably because water vaporized faster than glycerol as the reactants move through the spiral in the hot zone, causing a decrease in steam-to-carbon ratio. Finally it was decided to move on with the 1/16" straight pipe in Figure 3.3.



Figure 3.4. Reaction Section of Glycerol Steam Reforming Sytem.

The furnace used in this study (PROTHERM PZF 12/50/500) has three zones each of which has separate temperature controllers. In the upper (first) zone of the furnace, sprayed glycerol-water mixture is vaporized. The temperature of this zone is set to between 310-350 °C to guarantee complete vaporization of water and glycerol, as the latter has a boiling point of 290 °C at 1 atm. As the vaporized reactants and N_2 move through the quartz reactor in the furnace, they reach the middle (second) zone of the furnace, where the catalyst coated microreactor (see Section 3.3.3 for details) is present. The temperature of the middle zone is set as the reaction temperature. The product and unreacted gases then enter the bottom (third) zone, where again the temperature is above 310 °C and no condensation occurs on the walls of quartz reactor. Because it is not possible for glycerol (with a boiling point of 290 °C) to move in the post-reactor tubings in gas phase, and in order to prevent condensation in the tubings, a cold trap is placed right below the quartz reactor, so that all of the unreacted glycerol (or any other heavy compounds) are knocked down.



Figure 3.5. Post-reaction Section of Glycerol Steam Reforming System.

Although most of the water is also trapped in this cold trap, another cold trap placed in the Dewar flask is added to the system before the products reach gas chromatographs for analysis. The second cold trap is used to guarantee complete removal of condensables, as their presence has adverse effects on gas chromatography settings. After the first cold trap and before the second one, there is a three way valve, which is used either to trap N_2 in the quartz tube, to send the gas to soap bubble meter for manual check of gas flows or to send the effluent gases to the gas chromatographs.



Figure 3.6. Gas Chromatographs Used in Glycerol Steam Reforming System.

During the experiments, the first datum is recorded in 30th minute after the reaction started, then each datum is taken in every 45 minutes. The reported results belong to the arithmetic average of the data after the system reaches the state, which approximately corresponds to the 120th minute of the experiment.

3.2.4. Product Analysis System

The product stream consists of -on dry basis- inert N_2, H_2, CO, CH_4, CO_2, C_2H_4 and C_2H_6, all of which are detected and quantified using two different packed columns in two different gas chromatographs. H_2, N_2, CH_4 and CO are detected by Shimadzu GC-2014 gas

chromatograph, equipped with a Molecular Sieve 5A column and a thermal conductivity detector (TCD). N_2, CH_4, CO_2, C_2H_4 and C_2H_6 are detected by Shimadzu GC-8A gas chromatograph, equipped with a Porapak Q column and a TCD. The stream coming from the cold trap is sent continuously to Shimadzu GC-8A and after gas sampling, the flow is diverted to Shimadzu GC-2014. After a minute to let the sampling loop of GC-2014 get filled by the product gas stream, the sample is taken and analyzed. Sampling in both units is carried out by six-way valves that are set to inject 1 mL of gas sample to each chromatograph. Gas chromatograph parameters are listed in Table 3.3.

Before the experiments the calibrations of both gas chromatographs are done either by injecting known volumes of the species separately to the columns or feeding the gas chromatographs with gas mixtures with exact volumetric compositions set by the mass flow controllers, which are already calibrated. In the chromatographs, each gas forms a peak at specific retention times and the area under these peaks are calculated by integrator software. Micromole versus peak area graphs are plotted and the calibration curves are constructed as presented in Appendix B.

Table 3.3. GC conditions for product gas analysis.

GC Parameter	**Shimadzu GC-2014**	**Shimadzu GC-8A**
Detector type	Thermal conductivity	Thermal conductivity
Column oven temperature	50 °C	90 °C
Injector temperature	80 °C	90 °C
Detector temperature	150 °C	150 °C
Carrier gas	Argon	Helium
Carrier gas flow rate	25 mL.min^{-1}	25 mL.min^{-1}
Detector current	50 µA	120 µA
Column packing material	Molecular Sieve 5A (60-80 mesh)	Porapak Q (80-100 mesh)
Column tubing material	Stainless steel	Stainless steel
Column ID & length	1/8" OD x 2 m	1/8" OD x 3 m
Sampling loop	1 mL	1 mL

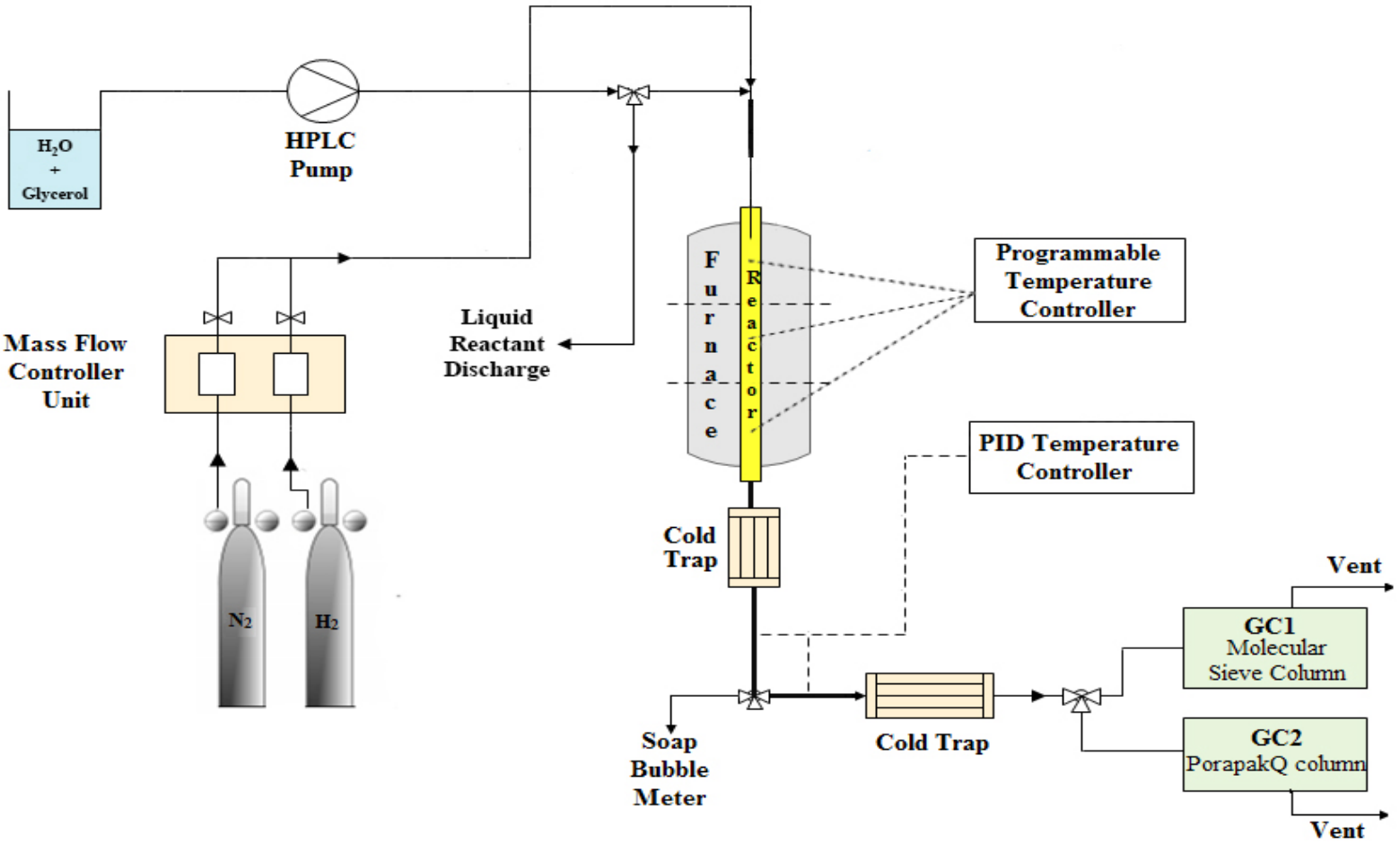

Figure 3.7. Schematic Diagram of the Reaction System.

3.3. Catalyst Preparation and Pretreatment

In this study, Rh/Al_2O_3, Pt/Al_2O_3 and Ru/Al_2O_3 catalysts are prepared and tested for catalytic activity in glycerol steam reforming. All catalysts are prepared by incipient to wetness impregnation method. Catalyst preparation includes support preparation, active catalyst preparation, microchannel coating and pretreatment steps.

3.3.1. Preparation of Support

Steam reforming of glycerol in this study takes place at a maximum of 600 °C. Therefore, the catalyst support must have high surface areas as well as high thermal stabilities. One of the frequently used support materials is γ-Al_2O_3 due to its high surface area (ca. 150-200 m^2/g). The maximum reaction temperature (600 °C) is not very high when it comes to steam reforming, but it has been reported that γ-Al_2O_3 has low stability at temperatures above 600 °C. It also has a tendency to promote carbon formation because of its acidic characteristic (Ma, 1995). Although the most thermally stable phase of alumina is the α phase, which is obtained by bringing γ-Al_2O_3 up to 1127 °C, low surface area of α phase causes low dispersion of active metals over the support (Doesburg et al., 1999). Therefore, an intermediate phase, which is called δ-phase, is created with high thermal stability and relatively high surface area. Three different procedures were investigated by Avci and co-workers (2004) with various drying and calcination temperatures and durations. The procedure and the BET surface areas of resulting materials are given in Table 3.4.

Table 3.4. Alumina support preparation procedures.

Procedure	**BET surface area (m^2g^{-1})**
Calcination at 1000 °C for 4 h	46.8
Drying of alumina at 150 °C for 2 h Calcination at 900 °C for 4 h	81.6
Drying of alumina at 105 °C for 16 h Calcination at 875 °C for 4 h	73.2

It is shown that the second procedure resulted in the highest BET surface area. From comparison of these procedures, it is clear that the duration of drying affects the BET surface area. Longer period of drying at a lower temperature gave a lower surface area, even though the calcination temperature was 25 °C below that of the second procedure. For the synthesis of all three microchannel catalysts used in this study, 3-μm sized γ-Al_2O_3 are dried at 150 °C for 2 hours and calcined at 900 °C for 4 hours in accordance with the procedures shown in table above.

3.3.2. Preparation of Active Catalysts

2 wt.% Rh/Al_2O_3, 2 wt.% Pt/Al_2O_3 and 2 wt.% Ru/Al_2O_3 catalysts are prepared using incipient-to-wetness impregnation method, which is a frequently used technique in catalyst synthesis. 2 grams of each catalyst are prepared.

When preparing the 2 wt.% Rh/Al_2O_3 catalyst, the amounts of Rh and Rh-containing salt ($Rh(NO_3)_3$, Sigma-Aldrich) are calculated and the solution containing Rh salt is put into a beaker. Deionized water is added into the beaker, until the total amount in the beaker is 2.353 mL (ca. 1.2 $mL_{solution}\ g^{-1}_{support}$). 2 wt.% Pt/Al_2O_3 preparation similarly starts with dissolving the calculated amount of Pt salt ($[Pt(NH_3)_4]\ (NO_3)_2$, Sigma-Aldrich) in certain amount of water (1.21 $mL_{solution}\ g^{-1}_{support}$). 2 wt.% Ru/Al_2O_3 preparation is slightly different than others, as there is no need for water addition. Ru is only 1.5 wt.% in its solution (Table 3.1), so the calculated amount of Ru solution is 2.489 mL for 2 grams of 2 wt.% Ru based catalyst. This amount is equal to 1.27 $mL_{solution}\ g^{-1}_{support}$, which is enough for incipient-to-wetness impregnation technique.

Once the solution is ready, the dried and calcined alumina support is mixed ultrasonically for 30 minutes under vacuum in a Buchner erlen. With the help of a peristaltic pump, the solution of metal precursor is impregnated over the support (Figure 3.1). The solution must be impregnated over the support as homogeneous as possible. The resulting slurry is mixed ultrasonically for 90 minutes under vacuum. After the mixing, it is dried at 120 °C for 16 hours. As the last step of preparation, the catalyst is crushed to obtain finer particles and it is calcined at 500 °C for 3 hours.

3.3.3. Catalyst Coating on Microchannel Plates

The preparation of catalytic microchannels is a process that requires some mechanical and chemical treatment. First, a 310-grade stainless steel cylindrical housing with a diameter of 18.6 mm and a length of 30 mm is manufactured by wire electrodischarge machining technique. In the middle of this housing, there is a proper gap that allows gas flow over the FeCrAlY plates when inserted (Figure 3.3). The diameter of the housing is set so that when it is inserted into the quartz reactor, no by-pass streams occur and the gas travels through the housing. FeCrAlY plates (Goodfellow) are obtained having the dimensions 2 mm x 5 mm x 20 mm. These plates are rasped to fit the housing and their widths are reduced to 4 mm, before any chemical treatment. Once the plates fit in the housing, without being too loose in it, they are cleaned with distilled water, ethanol and acetone and then calcined in furnace at 900 °C for 2 hours to enhance the adhesion of the coated plates by forming a native alumina layer on the plates.

In order to coat the plates with catalysts prepared (Section 3.3.2), the catalyst powder is mixed with a few drops deionized water at a water-to-powder ratio of 5 : 1. The resulting slurry is blade coated onto the plates till the weight per surface area reaches ca. 0.02 $g_{cat}cm^{-2}$. The slurry is coated onto the plate while still wet, so it is a challenge to estimate the dry weight of catalyst per surface area. Although it depends on the amount of water added to the powder, the weight of the coated slurry must be around 0.035-0.040 $g_{cat}cm^{-2}$ to reach the dry weight per surface area of 0.02 $g_{cat}cm^{-2}$. The coated catalysts must have the same height on the plate and it must be inserted into the housing while still wet, in order to sweep the excess catalyst slurry present on the edges. Otherwise, when the solid catalyst coating is inserted into the housing, the catalyst coated on the edges may crack.

The catalyst coated plates are dried at 120 °C for 16 hours and they are calcined at 500 °C for 3 hours. After the calcination step, catalytic plates are ready for use. They are weighed before using to determine the exact amount of catalyst present on the plate. Then, the plate is inserted back into the housing, and a piece of quartz wool is stuck into the housing as well to stabilize the plate in the housing. Figure 3.3 gives a visual idea of the structure of coated plate and housing.

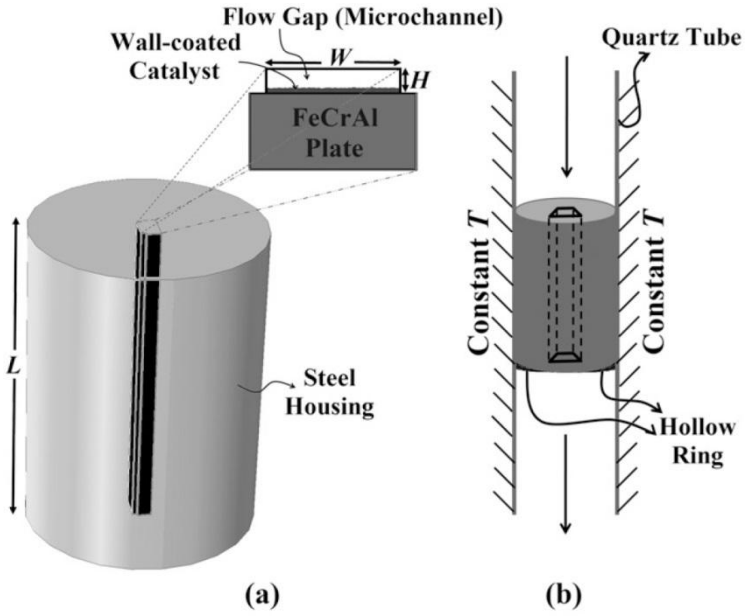

Figure 3.8. Microreactor Configuration a. Coated Microchannel Reactor b. Location of Steel Housing in Quartz Tube (Karakaya *et al*., 2012).

3.3.4. Pretreatment

Coated catalysts must be activated after calcination process. The reason for pretreatment is to reduce the active metals from their oxidized states, which occurs after calcination, to metallic states. In order to achieve that, 40 NmL min^{-1} H_2 flow is passed over the catalysts at 800 °C for 2 hours in situ before the reaction tests.

3.4. Reaction Tests

3.4.1. Blank Tests

In order to ensure that the materials of construction (stainless steel tubings, 310-grade stainless steel housing, quartz reactor, FeCrAlY and quartz wool) are inert towards the reactants, blank tests are conducted under reaction conditions. However, an activity is observed in the blank test conducted at 425 °C, the lowest value of temperature scale investigated in this study. As glycerol decomposition rate increases with temperature (from 425 °C to 600 °C), an activity seen at 425 °C is a strong indicator that at least that activity observed in blank tests is expected to increase at higher temperatures.

Another blank experiment is conducted to determine the source of the activity. This time, housing and plate are taken out of the reaction system. In a reaction system that consisted of stainless steel tubing, quartz reactor and quartz wool, no activity is observed. A third blank experiment is made to see whether the housing or the plate is responsible for the activity. This time only housing is inserted into the quartz reactor, without the plate inside. When compared to the first experiment, small catalytic activity is observed. It is concluded that the stainless steel housing and FeCrAlY plates are not inert towards the reactants at 425 °C.

Table 3.5. List of blank tests in microchannel reactor.

#	Temp. (°C)	Gly./H_2O/N_2 (molar ratio)	S/C	Liquid mixture feed ($mL.min^{-1}$)	N_2 gas feed ($NmL.min^{-1}$)	Total gas flow ($NmL.min^{-1}$)
1	425	1 / 15 / 16	5	0.0421	48	96
2	450	1 / 15 / 16	5	0.0421	48	96
3	475	1 / 15 / 16	5	0.0421	48	96
4	500	1 / 15 / 16	5	0.0421	48	96
5	550	1 / 15 / 16	5	0.0421	48	96
6	600	1 / 15 / 16	5	0.0421	48	96

In order to determine the degree of activity at different temperatures, blank tests are conducted at different temperatures between 425-600 °C. List of experiments for blank tests are summarized in Table 3.5. Outcomes of the blank tests are given and discussed in Chapter 4.

3.4.2. Steam Reforming of Glycerol in Microchannel Reactor

Gas phase glycerol steam reforming experiments are conducted using quartz tube involving the housing and the 2 wt.% precious metal over alumina catalyst coated plate. Coated plates are inserted into the housing and a small piece of quartz wool is inserted into the bottom of the housing to stabilize the position of the plate in the housing. Before the housing is placed in the quartz reactor, quartz wool with a thickness of approximately 1.0

cm is stuck on top of a hollow ring in the middle of the quartz reactor (Figure 3.3b, 1 cm thick quartz wool that is placed between the ring and the housing is not shown). This design keeps the housing stationary at the desired position and prevents bypass through annulus between the housing and the quartz tube. During the experiments, bypass streams are diminished thanks to the thermal expansion of the 310-grade steel housing at high temperatures. After the housing is placed on the quartz wool, another 1.0 cm-thick quartz wool is placed on top of the housing (not shown in Figure 3.3b). This piece of quartz wool is necessary in reactions with high coking rate, like glycerol steam reforming, in order to understand whether coking occurs before reactants reach the catalytic zone. Temperatures of three zones in the furnace are controlled separately with three separate PID controllers. The measurement is done with the precision of ±1.0 °C. Once the desired temperature is reached, the temperature of each zone stays constant with deviations of ±2.0 °C.

Glycerol steam reforming experiments are conducted to investigate the effects of temperature, steam-to-carbon ratio, total flow and reactant dilution ratio with inert (N_2) on the reaction. At different temperatures, steam-to-carbon molar ratio is kept constant at 5, reactant-to-inert molar ratio at 1 and total flow at 96 NmL min^{-1} during each experiment. At different steam-to-carbon ratios, the temperature is kept constant at 500 °C and 600 °C for Rh-based catalyst, reactant-to-inert molar ratio at 1 and total flow at 96 NmL min^{-1} during each experiment (experiments 4, 6, 10, 15, 17-24 in Table 3.6). Effect of total flow is investigated over Rh/Al_2O_3 catalyst, keeping the temperature constant at 600 °C, reactant-to-inert molar ratio at 1 and steam-to-carbon molar ratio at 5 (experiments 6, 25 and 26 in Table 3.6). Finally, the effect of reactant dilution is studied over Rh/Al_2O_3 catalyst at 600 °C, steam-to-carbon molar ratio equals 5 and a total flow of 96 NmL min^{-1} (experiments 6 and 27 in Table 3.6). A full list of experiment with varying parameters is given in Table 3.6.

In the calculations, all liquid intermediate products are neglected. Glycerol conversions are based on the glycerol entering the system and number of moles of carbon containing species detected by Molecular Sieve 5A and Porapak Q columns (CH_4, CO, CO_2, C_2H_4 and C_2H_6). All values reported in Section 4 are calculated on dry basis. As glycerol contains three moles of carbon atoms, the glycerol conversion is calculated as stated in Eq. 3.1 (Nichio *et al.*, 2010).

Table 3.6. List of experiments for parametric study of glycerol.

#	Catalyst	T (°C)	S/C	Liquid feed (NmL min^{-1})	N_2 feed (NmL min^{-1})	Total flow (NmL min^{-1})
1	2 wt.% Rh/Al_2O_3	425	5	0.0421	48	96
2	2 wt.% Rh/Al_2O_3	450	5	0.0421	48	96
3	2 wt.% Rh/Al_2O_3	475	5	0.0421	48	96
4	2 wt.% Rh/Al_2O_3	500	5	0.0421	48	96
5	2 wt.% Rh/Al_2O_3	550	5	0.0421	48	96
6	2 wt.% Rh/Al_2O_3	600	5	0.0421	48	96
7	2 wt.% Pt/Al_2O_3	425	5	0.0421	48	96
8	2 wt.% Pt/Al_2O_3	450	5	0.0421	48	96
9	2 wt.% Pt/Al_2O_3	475	5	0.0421	48	96
10	2 wt.% Pt/Al_2O_3	500	5	0.0421	48	96
11	2 wt.% Pt/Al_2O_3	600	5	0.0421	48	96
12	2 wt.% Ru/Al_2O_3	425	5	0.0421	48	96
13	2 wt.% Ru/Al_2O_3	450	5	0.0421	48	96
14	2 wt.% Ru/Al_2O_3	475	5	0.0421	48	96
15	2 wt.% Ru/Al_2O_3	500	5	0.0421	48	96
16	2 wt.% Ru/Al_2O_3	600	5	0.0421	48	96
17	2 wt.% Rh/Al_2O_3	500	4	0.0355	57	96
18	2 wt.% Rh/Al_2O_3	500	3	0.0288	66	96
19	2 wt.% Rh/Al_2O_3	600	4	0.0355	57	96
20	2 wt.% Rh/Al_2O_3	600	3	0.0288	66	96
21	2 wt.% Pt/Al_2O_3	500	4	0.0355	57	96
22	2 wt.% Pt/Al_2O_3	500	3	0.0288	66	96
23	2 wt.% Ru/Al_2O_3	500	4	0.0355	57	96
24	2 wt.% Ru/Al_2O_3	500	3	0.0288	66	96
25	2 wt.% Rh/Al_2O_3	600	5	0.0562	64	128
26	2 wt.% Rh/Al_2O_3	600	5	0.0702	80	160
27	2 wt.% Rh/Al_2O_3	600	5	0.0632	24	96

$$X_{glycerol} = 100 \times \frac{\text{moles of carbon in gaseous products}}{3 \times \text{moles of glycerol in the feed}} \quad (3.1)$$

Selectivity of each species is calculated by dividing the molar amount of the gaseous species in the product stream by the molar amount of glycerol converted:

$$\text{Selectivity}_i = \frac{\text{moles of species "i" in gaseous products}}{\text{moles of glycerol converted}} \quad (3.2)$$

4. RESULTS AND DISCUSSION

This study presents the results of a parametric study on glycerol steam reforming. The parameters investigated are temperature, steam-to-carbon ratio (over Rh, Pt and Ru catalysts), total flow and reactant dilution (over Rh catalyst). All the catalysts used in all experiments are 2 wt.% of precious metal supported on δ-alumina, that are blade-coated on FeCrAlY plates. The results of blank tests at different temperatures are also shown, as the reaction system without the catalyst is not inert towards reactants. Glycerol conversions and gaseous product selectivities are reported for each experiment. SEM and EDX analysis results of reduced and spent Rh/Al_2O_3, catalysts are also reported to point out the changes on catalyst surface and active metallic sites after they are exposed to reaction conditions.

4.1. Effect of Temperature

Temperature is a key parameter to all steam reforming reactions. In this study, glycerol steam reforming experiments are conducted over three different catalysts at temperatures between 425 °C and 600 °C. Steam-to-carbon ratio, N_2 flow rate and total flow rate are kept constant at 5, 48 NmL min^{-1} and 96 NmL min^{-1}, respectively.

Glycerol conversion is calculated by Equation 3.1. Any liquid products are neglected when calculating the conversion. In order to see the effect of the microchannel reactor components (housing and FeCrAlY plate) on the reaction, the results of blank tests are also presented. Experiments are conducted at six different temperatures over Rh catalyst and blank plates and at five different temperatures over Pt and Ru catalysts. The results show that conversion is a strong function of temperature. At temperatures less than 500 °C, Ru, Pt and blank experiments show conversions less than 1%. In the same temperature range, Rh catalyst showed conversions between 1% and 3%. Conversion levels increased with increasing temperature. At 550 °C, conversions obtained by blank plate and Rh catalyst are 3% and 5%, respectively. As the temperature is further increased to 600 °C, conversions increased drastically. Conversion was 24% over Rh and in other three cases conversions turned out to be around 15%. Surprisingly, conversion obtained by blank experiment is found to be slightly higher than those of Pt and Ru catalysts at 600 °C.

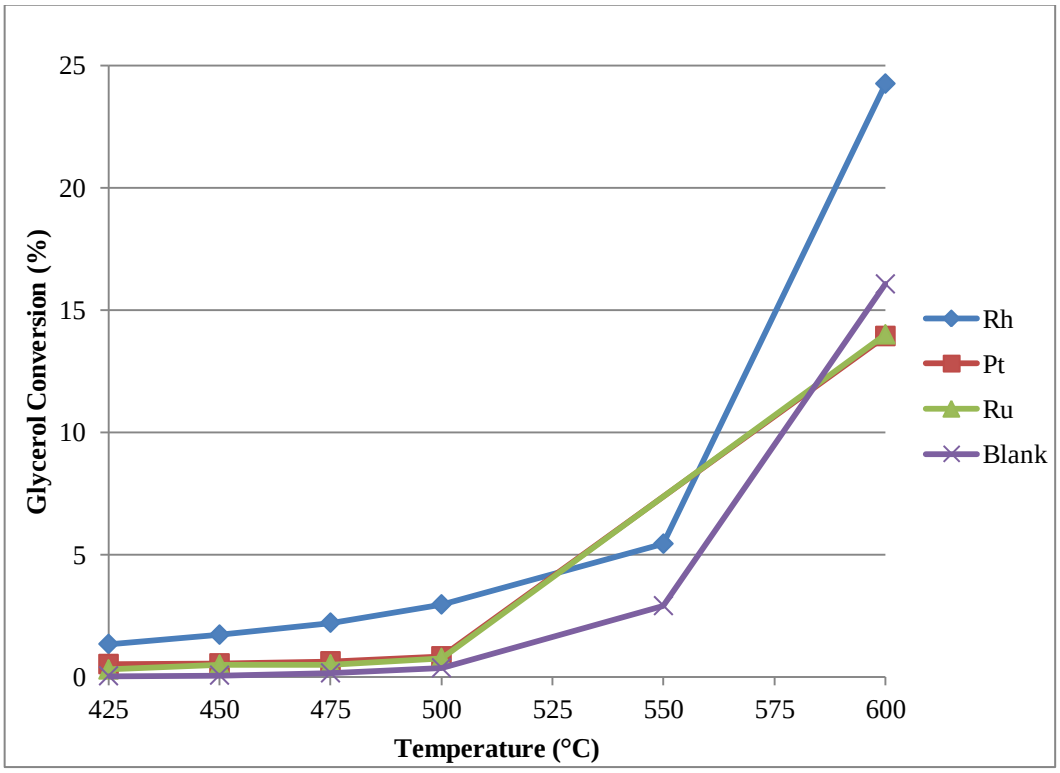

Figure 4.1. Glycerol Conversion vs Temperature (S/C=5, N_2 flow: 48 NmL min^{-1}, Total flow: 96 NmL min^{-1}).

Positive correlation of conversion with temperature is an expected trend. Steam reforming is an endothermic reaction, so when the heat input is increased, steam reforming reaction shifts towards the products, which ends up with increased glycerol conversion. Rh is apparently the best performing catalyst at all temperatures, giving the highest conversion levels. Blank test conversion levels are less than those of Pt and Ru catalysts up to 500 °C, but, at 600 °C, blank plate outclasses Pt and Ru. Although the metal housing and plate do not contain any precious metals, they are still active towards glycerol steam reforming reaction. The plate has iron (72.8%), chromium (22.0%) and aluminum (5.0%) and the 310-grade metal housing has about 25% chromium and 20% nickel in their structure (Goodfellow, 2014; Sandmeyer, 2014). Especially nickel is well known with its activity in steam reforming reactions. Therefore, it is possible to see some activity even at low temperatures and more activity at high temperatures.

There are six gaseous products detected as the results of glycerol steam reforming reaction. These are H_2, CH_4, CO, CO_2, C_2H_4 and C_2H_6. Selectivities of these products are

compared with each other at different temperatures. Selectivity is defined as the ratio of the moles of product to moles of glycerol converted. In this study, selectivity of a product is calculated as shown in Equation 3.2.

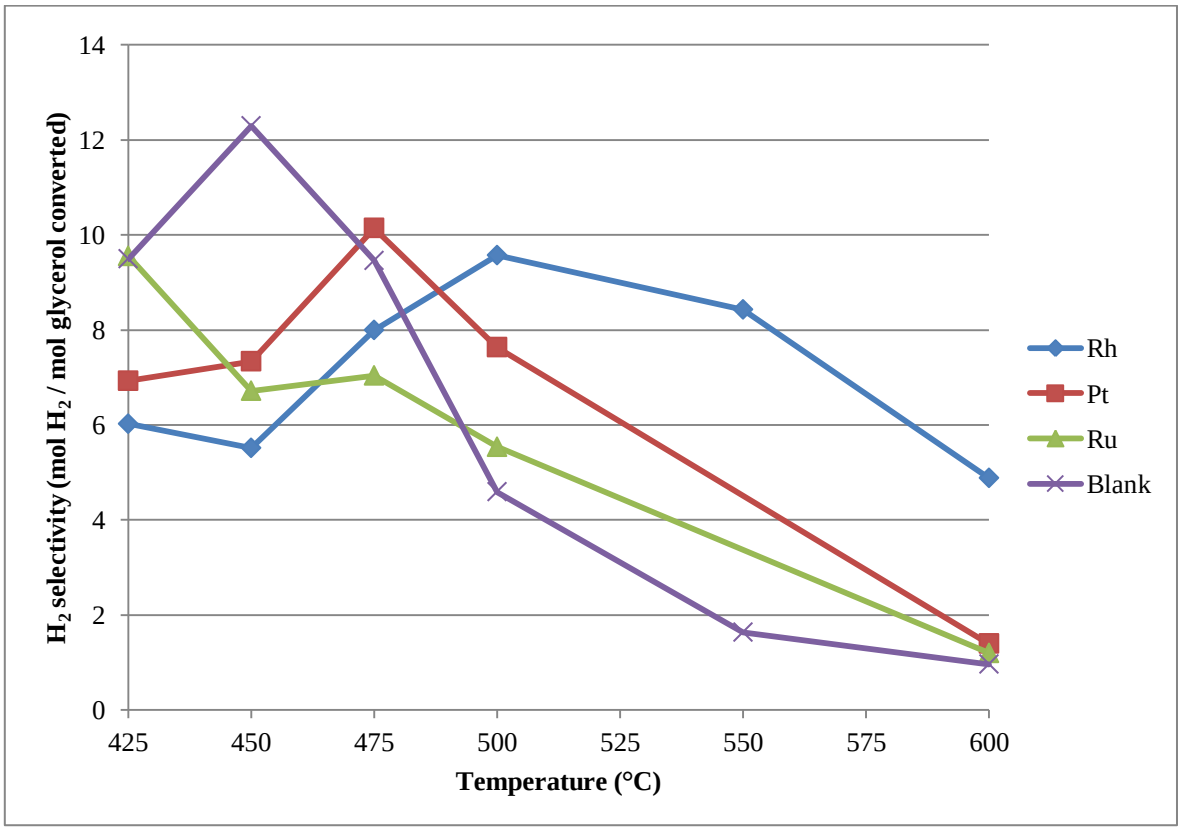

Figure 4.2. H_2 Selectivity vs Temperature (S/C=5, N_2 flow: 48 NmL min^{-1}, Total flow: 96 NmL min^{-1}).

In glycerol steam reforming mechanism, there are three major sources of H_2 produced. First one is the pyrolysis of glycerol to CO and H_2 (Reaction 2.1), which is the first step of the steam reforming reaction. H_2 can also be produced as a result of water gas shift (Reaction 2.2), where CO and water react to give H_2 and CO_2. These two reactions are common for all types of steam reforming reactions. Additionally, for glycerol steam reforming case, dehydrogenation (Reaction 2.10) takes place. Glycerol itself or intermediate products produced from glycerol may be dehydrogenated. H_2 selectivities obtained from different catalysts at different temperatures, shown in Figure 4.2, must therefore be evaluated by considering the selectivities of other products and it is very difficult to determine which reaction is dominant. For three different catalysts and the

blank cases, as the temperature increases, H_2 selectivity does not increase. Between 425 °C and 600 °C, maximum H_2 selectivities are achieved at different temperatures and then the selectivities start to decrease with increasing temperature. In the blank experiment, H_2 selectivity is maximum at 12 at 450 °C, and it is around 10 at 425 °C and 475 °C. With increasing temperature, H_2 selectivity decreases sharply. Ru shows maximum H_2 selectivity at 425 °C. It decreases with temperature down to 1 at 600 °C. Pt catalyst reaches maximum H_2 selectivity of 10 at 475 °C and sharply decreases after 500 °C. Rh catalyst shows maximum H_2 selectivity of 9.5 at 500 °C and it decreases with increasing temperature, reaching the value 5 at 600 °C. The H_2 selectivity obtained over Rh catalyst does not go below 5 at any temperature between 425 °C and 600 °C.

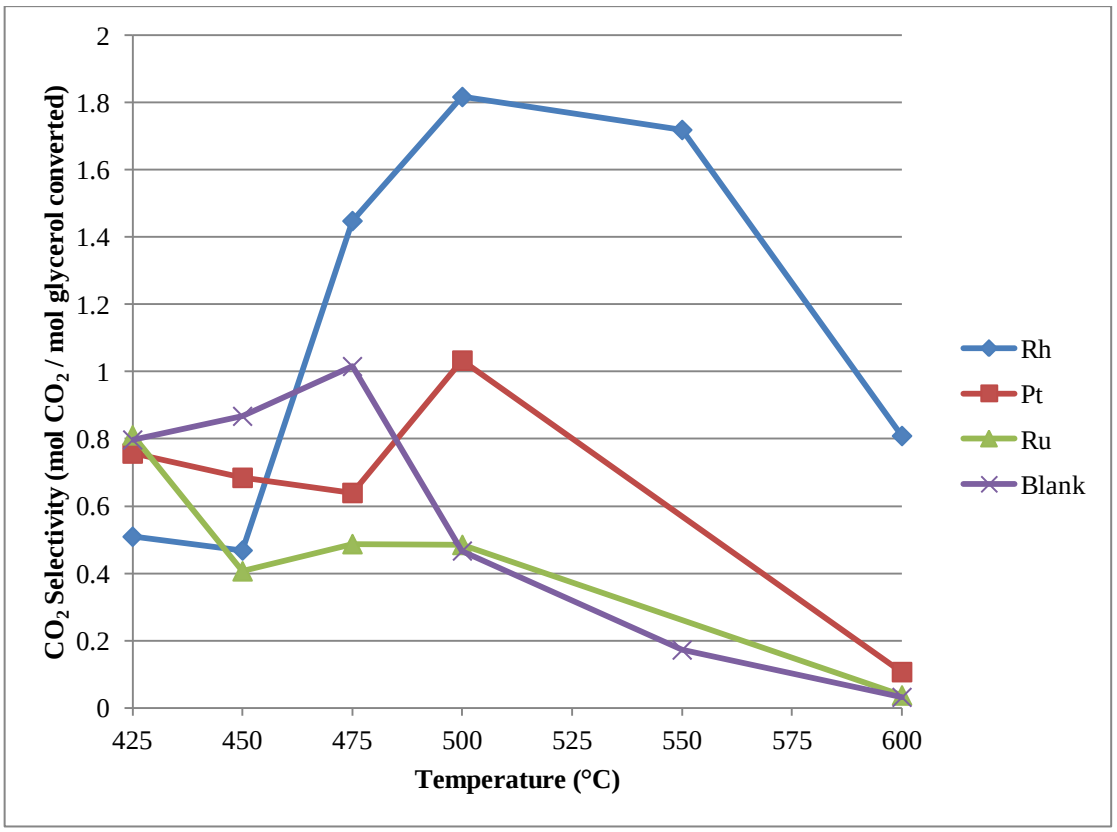

Figure 4.3. CO_2 Selectivity vs Temperature (S/C=5, N_2 flow: 48 NmL min^{-1}, Total flow: 96 NmL min^{-1}).

The change in CO_2 selectivity with temperature over the three catalysts and in the blank tests is shown in Figure 4.3. In general, at the points where H_2 selectivity is high, CO_2 selectivities are also high. H_2 and CO_2 selectivities show similar trends with

temperature. This trend is observed for all three different catalysts and the blank plate. Same behavior observed for H_2 and CO_2 selectivities may be a result of the water gas shift reaction. As there is no external oxygen source into the reaction system and there is no mechanism suggesting CO_2 removal as a side product, it is believed that CO_2 production is a result of water gas shift reaction only. The domination of water gas shift reaction explains the similar trend of H_2 and CO_2 selectivities. Water gas shift reaction is a slightly exothermic reaction. At lower temperatures reaction kinetics may dominate, so until some point, an increase in H_2 and CO_2 production is observed. After some point, which is different for four cases in this study, reaction is thermodynamically controlled and a decrease in H_2 and CO_2 production is observed with increasing temperature.

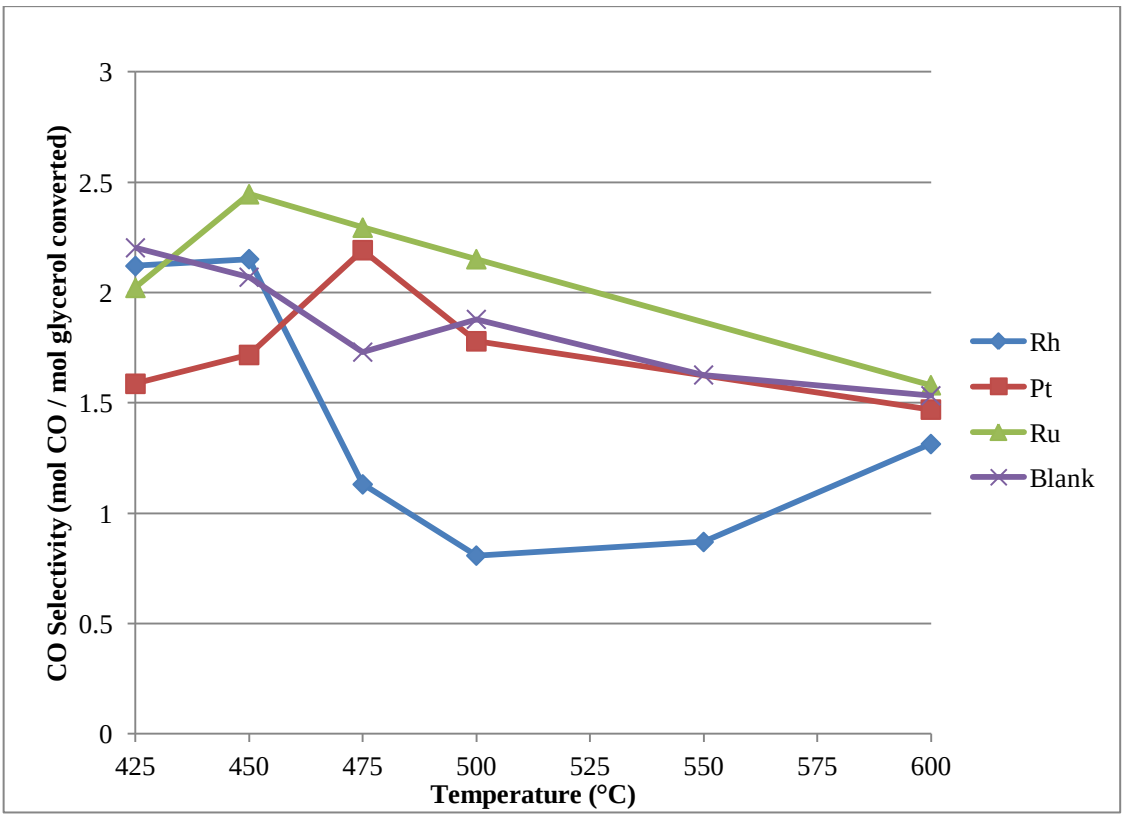

Figure 4.4. CO Selectivity vs Temperature (S/C=5, N_2 flow: 48 NmL min^{-1}, Total flow: 96 NmL min^{-1}).

The change in CO selectivity with temperature over the three catalysts and in the blank tests is shown in Figure 4.4. CO selectivity shows slight decrease with temperature for Pt coated, Ru coated and blank plates between values 2.5 and 1.5. Pt and Ru catalysts

show their maximum CO selectivities at temperatures 475 °C and 450 °C, respectively. These maximum CO selectivities, however, are not much higher than the rest of CO selectivities obtained at different temperatures. The effect of temperature on CO selectivity is best observed by investigating the behavior of the Rh/Al_2O_3 catalyst, on which the CO selectivity shows a parabolic behavior with increasing temperature. At low temperatures, CO selectivity is around 2.2. At 500 °C, CO selectivity hits a minimum of 0.8, and the selectivity then starts to increase with temperature. This trend is the opposite of H_2 and CO_2 selectivities. Again in this case, water gas shift reaction may be responsible for this trend. As temperature increases above 500 °C, reaction may be controlled thermodynamically and water gas shift equilibrium may shift to the reactants side, which explains the opposite behavior of CO against H_2 and CO_2. Reactions 2.3 and 2.7 are the other sources of CO. Other than these two, CO removal reactions from glycerol or its intermediate products may be effective in changes in CO selectivity.

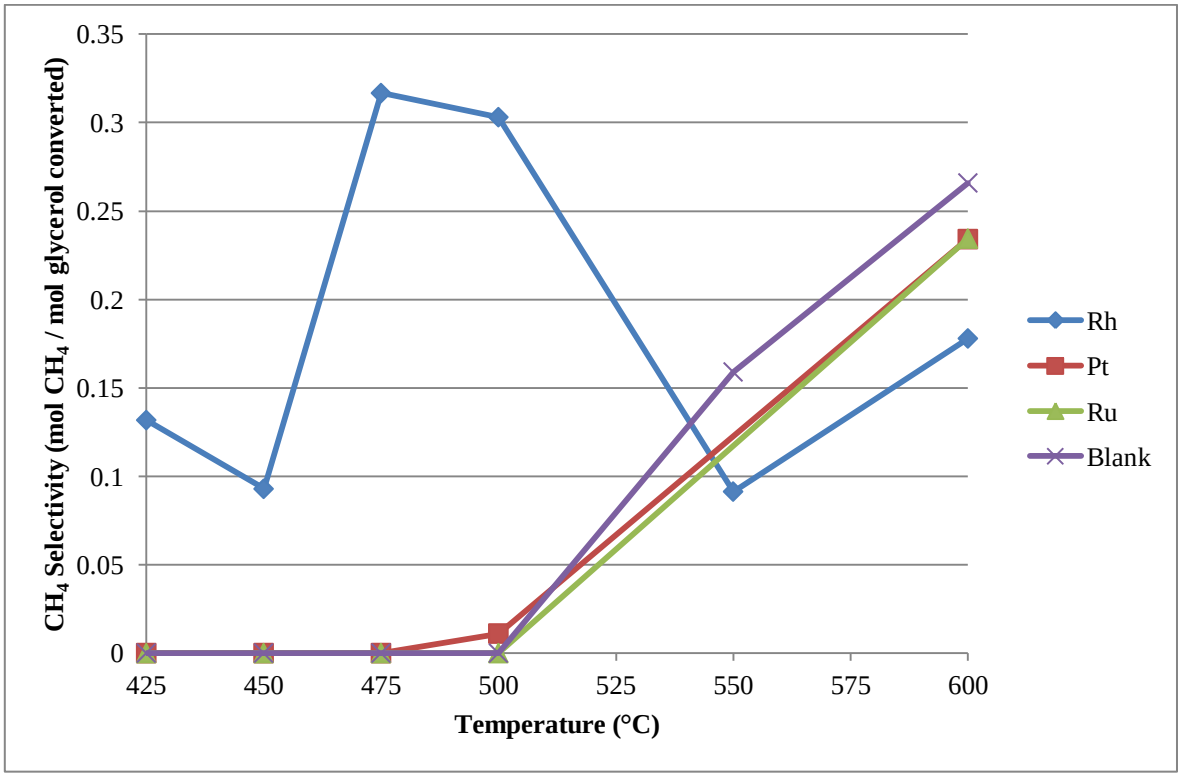

Figure 4.5. CH_4 Selectivity vs Temperature (S/C=5, N_2 flow: 48 NmL min^{-1}, Total flow: 96 NmL min^{-1}).

The change in CH_4 selectivity with temperature over the three catalysts and in the blank tests is shown in Figure 4.5. In the tests conducted over Ru and Pt coated catalysts and in the blank test, CH_4 selectivities turn out to be either zero or very close to zero. At 600 °C, CH_4 selectivities increase sharply to around 0.25. Rh based catalyst, however, gives CH_4 selectivity even at low temperatures and it gives maximum CH_4 selectivities at 475 °C and 500 °C. At higher temperatures, Rh gives less CH_4 selectivity compared with other catalysts. Reactions 2.4, 2.5 and 2.6 are the possible sources of CH_4. Additionally, dehydrogenation, dehydration and CO removal reactions occur during glycerol steam reforming which may end up with additional CH_4 produced (Lin, 2013).

$$C + 2H_2 \leftrightarrow CH_4 \quad (2.4)$$

$$CO + 3H_2 \leftrightarrow CH_4 + H_2O \quad (2.5)$$

$$CO_2 + 4H_2 \leftrightarrow CH_4 + 2H_2O \quad (2.6)$$

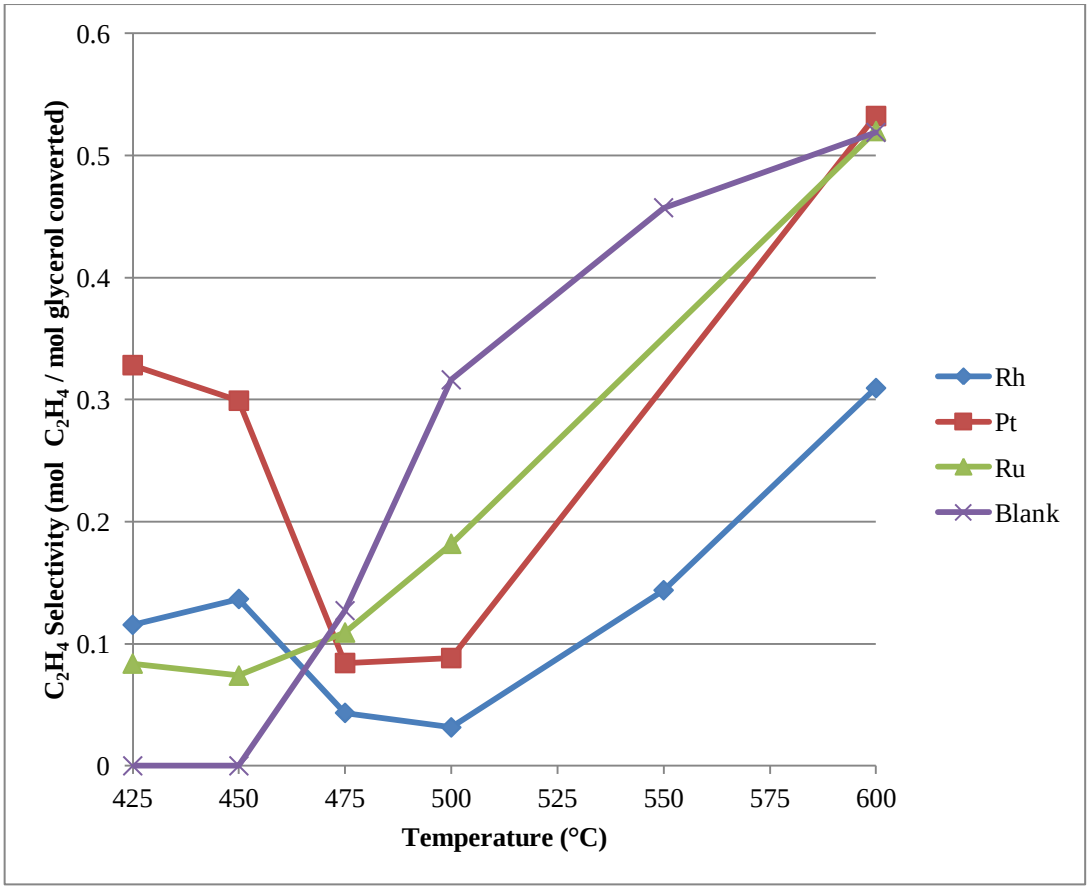

Figure 4.6. C_2H_4 Selectivity vs Temperature (S/C=5, N_2 flow: 48 NmL min^{-1}, Total flow: 96 NmL min^{-1}).

Although it is very complicated to discuss which reactions dominate at which temperature to increase or suppress CH_4 formation, it can be concluded that Rh catalyst has a different mechanism than those of other catalysts which is likely to cause high CH_4 selectivities at lower temperatures.

C_2H_4 and C_2H_6 selectivities, presented in Figures 4.6 and 4.7, respectively, show opposite behavior to H_2 and CO_2 selectivities as temperature changes. C_2H_4 and C_2H_6 are the by-products formed from (mostly liquid) intermediate products through dehydration, dehydrogenation and CO removal reactions (Lin, 2013). C_2H_4 and C_2H_6 selectivities increase at temperatures where H_2 selectivities decrease. At 600 °C, selectivities of C_2H_4 and C_2H_6 are at their maxima for four different cases. Rh catalyst gives less C_2H_4 selectivity than any other catalyst at temperatures above 475 °C. C_2-hydrocarbons further decompose to carbon, but Rh is resistant against carbon formation, so it adds up perfectly that C_2H_4 selectivity is less over Rh. Blank tests give the most C_2H_4 among all in the same temperature range. This is expected as Ni is the active metal in blank tests (20% Ni in housing) and Ni is very prone to coking.

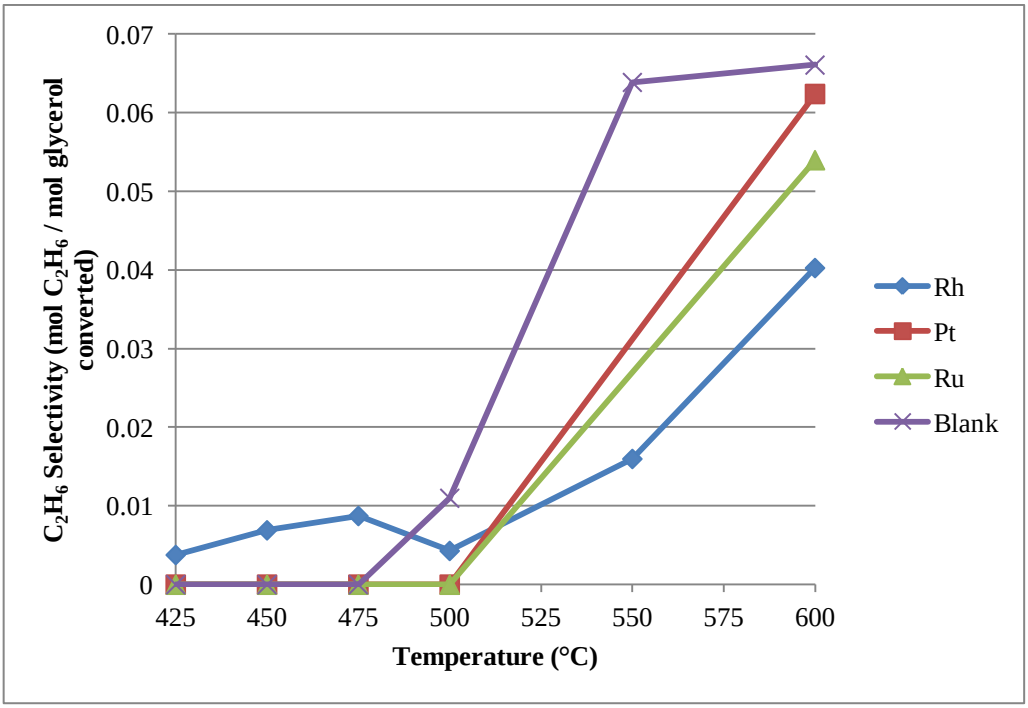

Figure 4.7. C_2H_6 Selectivity vs Temperature (S/C=5, N_2 flow: 48 NmL min^{-1}, Total flow: 96 NmL min^{-1}).

4.2. Effect of Steam-to-Carbon Ratio

Steam-to-carbon ratio is an important parameter in steam reforming reactions, as steam is a reactant itself. The effect of steam-to-carbon ratio is investigated at 500 °C with a total flow of 96 NmL min^{-1} over 2 wt.% Rh/Al_2O_3, 2 wt.% Pt/Al_2O_3 and 2 wt.% Ru/Al_2O_3 catalysts by adjusting the steam-to-carbon ratio to 3, 4 and 5. Additionally, effect of steam-to-carbon ratio over Rh catalyst is tested at 600 °C. Glycerol conversion and gaseous product selectivities obtained from each experiment are reported.

The effect of steam-to-carbon ratio on glycerol conversion is shown in Figure 4.8. As steam-to-carbon ratio increases, for Pt and Ru catalysts, glycerol conversion level does not change. Conversion levels stay constant between 0.6% and 1.0%. At 500 °C, Rh catalyst gives about 5% glycerol conversion when steam-to-carbon ratio is 3 and 4. When steam-to-carbon ratio is further increased to 5, glycerol conversion drops to 3%. Rh catalyst, however, shows an opposite trend at 600 °C. Glycerol conversion goes up from 16% to 22%, and then to 24% as steam-to-carbon ratio increases from 3 to 5.

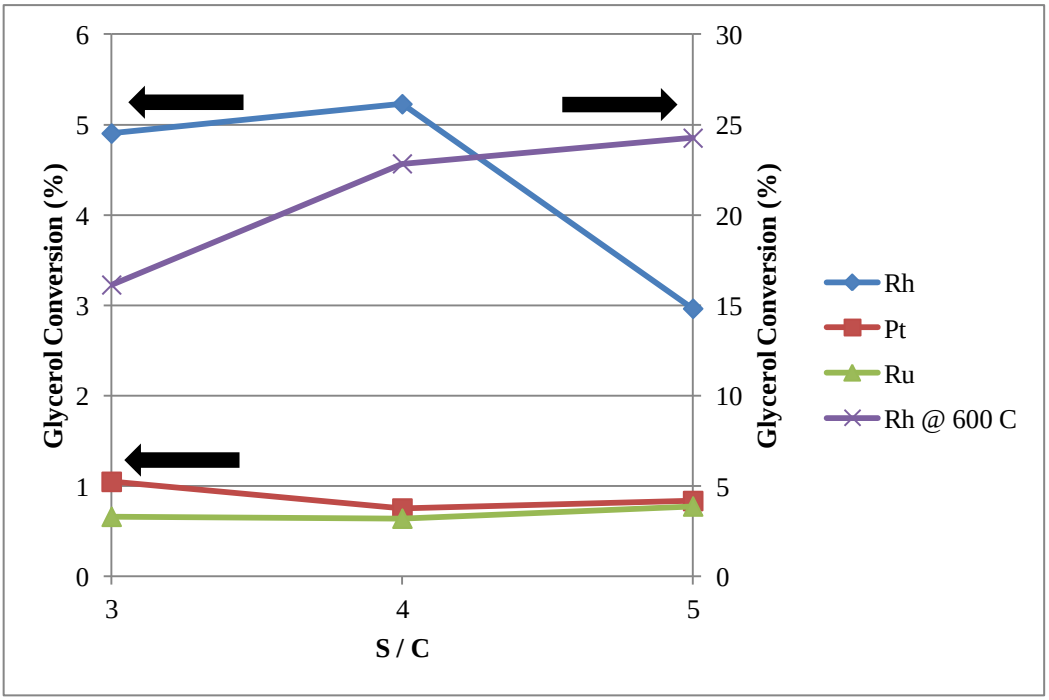

Figure 4.8. Glycerol Conversion vs Steam-to-Carbon Ratio.

Ru and Pt catalysts show very little conversions at 500 °C, so small fluctuations in conversion levels as steam-to-carbon ratio changes is not open to interpretation. In general, it can be concluded that 500 °C is not appropriate to observe any changes on glycerol conversion with steam-to-carbon ratio. Glycerol conversion obtained by Rh catalyst at the same temperature decreases by 2% as steam-to-carbon ratio is increased from 4 to 5. However, at 600 °C, glycerol conversion increases with increasing steam-to-carbon ratio. When the overall glycerol steam reforming reaction is considered, extra steam put into the system shift the reaction towards the products, which results in an increase in glycerol conversion. Apparently at different temperatures, two opposite scenarios are observed. Such a behavior can possibly be explained by the non-monotonic dependence of reaction rate on steam and by a possible change in the steam reforming mechanism over Rh with temperature.

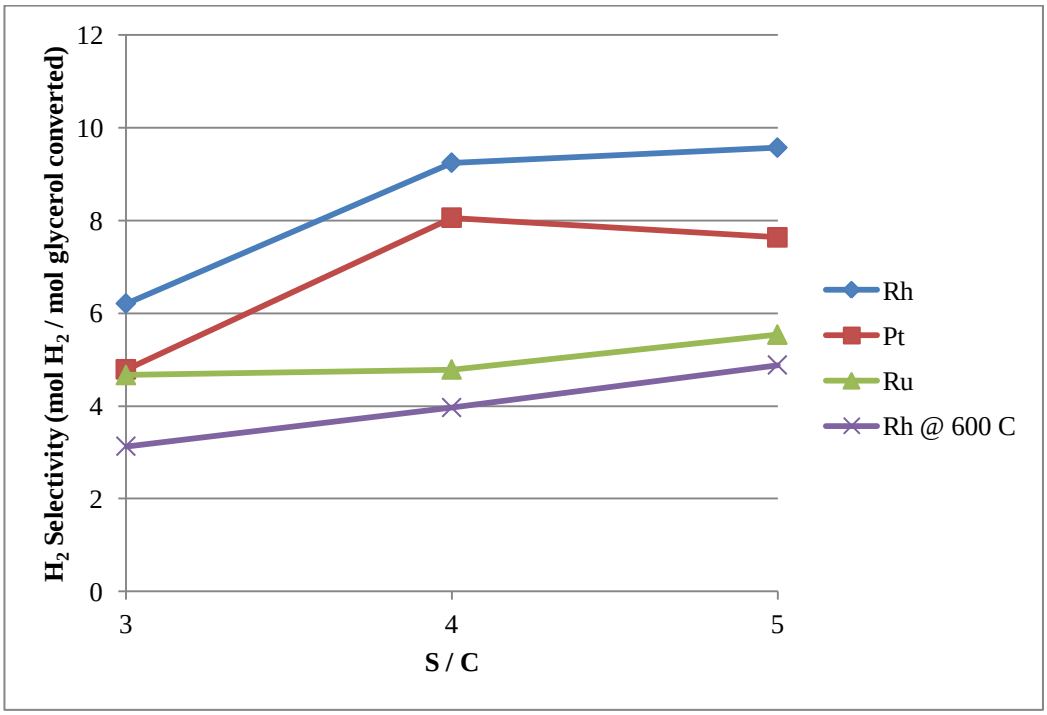

Figure 4.9. H_2 Selectivity vs Steam-to-Carbon Ratio.

H_2 selectivity, in general, increases with increasing steam-to-carbon ratio (Figure 4.9). At 500 °C, for Pt catalyst, there is a sharp increase of H_2 selectivity from 5 to 8 as steam-to-carbon ratio is increased from 3 to 4. For Ru catalyst, H_2 selectivity increases from about 4.5 to 5.5 as steam-to-carbon ratio is increased from 4 to 5. Rh catalyst

similarly shows an increase in H_2 selectivity from 6.0 to 9.2 as steam-to-carbon ratio increases from 3 to 4. At 600 °C, Rh catalysts exhibits similar behavior, where H_2 selectivity increases linearly from 3 to 5 as steam-to-carbon ratio is set to 3, 4 and 5. All data on H_2 selectivity suggest that an increase in steam-to-carbon ratio has positive effect on H_2 selectivity. This may be explained by the water gas shift reaction taking place. As more steam is put into the reaction system, water gas shift reaction is shifted towards the products' side, which favors H_2 production.

CO selectivity, except over Ru catalyst, decreases as steam-to-carbon ratio increases (Figure 4.10). In the experiments at 500 °C over Ru catalyst, CO selectivity stays constant at 2.1 as steam-to-carbon ratio changes. Over Pt catalyst at 500 °C and Rh catalyst at 600 °C, CO selectivity slightly decreases with increasing steam-to-carbon ratio. Rh catalyst at 500 °C gives CO selectivity of 2.0 when steam-to-carbon ratio is 3. CO selectivity sharply decreases to 0.9 at steam-to-carbon ratio equals 4, and then it shows a slight decrease to 0.8 as steam-to-carbon ratio is further increased to 5. A decreasing CO selectivity trend may be a result of the water gas shift reaction. An increase in steam feed shifts the water gas shift reaction towards the products, which results in an increase in H_2 and CO_2 selectivity and a decrease in CO selectivity.

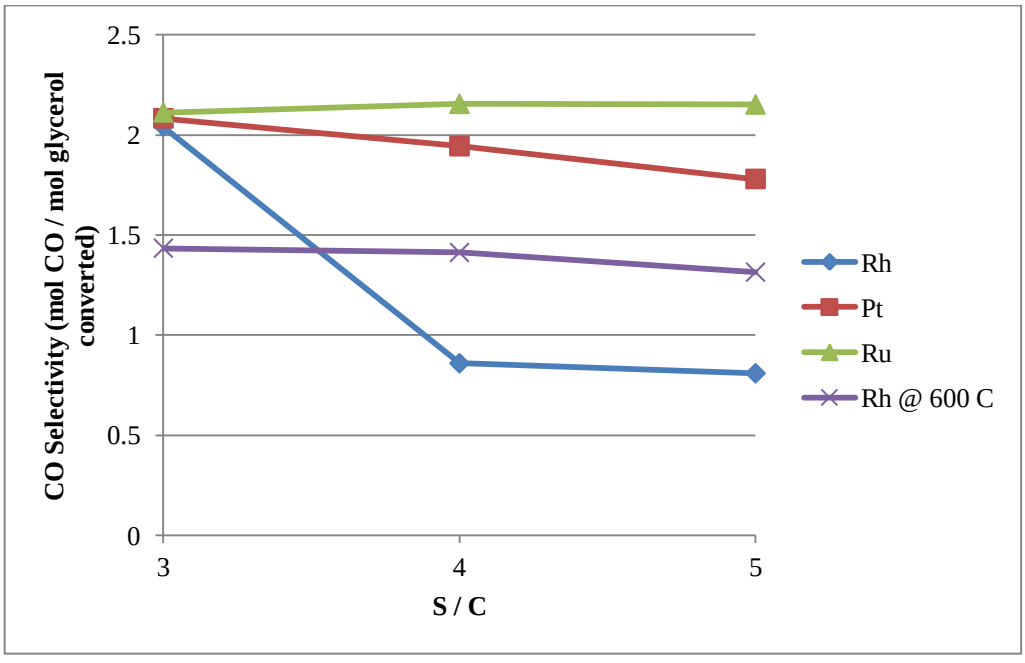

Figure 4.10. CO Selectivity vs Steam-to-Carbon Ratio.

The effect of steam-to-carbon ratio on CO_2 selectivity is shown in Figure 4.11. At 500 °C and 600 °C, for steam-to-carbon ratios 3, 4 and 5, over three different precious metal catalyst, CO_2 selectivity increases with increasing steam-to-carbon ratio. Over Rh catalyst at 500 °C, as steam-to-carbon ratio increases from 3 to 4, CO_2 sharply increases from 0.7 to 1.8. A further increase in steam-to-carbon ratio to 5 does not change the CO_2 selectivity. CO_2 selectivities over Pt at 500 °C and Rh at 600 °C show slightly increasing trends with increasing steam-to-carbon ratios. CO_2 selectivity stays constant at 0.4 as steam-to-carbon ratio increases from 3 to 4 over Ru catalyst. When steam-to-carbon ratio is equal to 5, Ru catalyst shows a minor increase in CO_2 selectivity to 0.5. As explained for H_2 and CO selectivity cases, water gas shift reaction may affect the CO_2 selectivity. As steam-to-carbon ratio increases, water gas shift reaction equilibrium shifts to the products' side, resulting an increase in CO_2 selectivity.

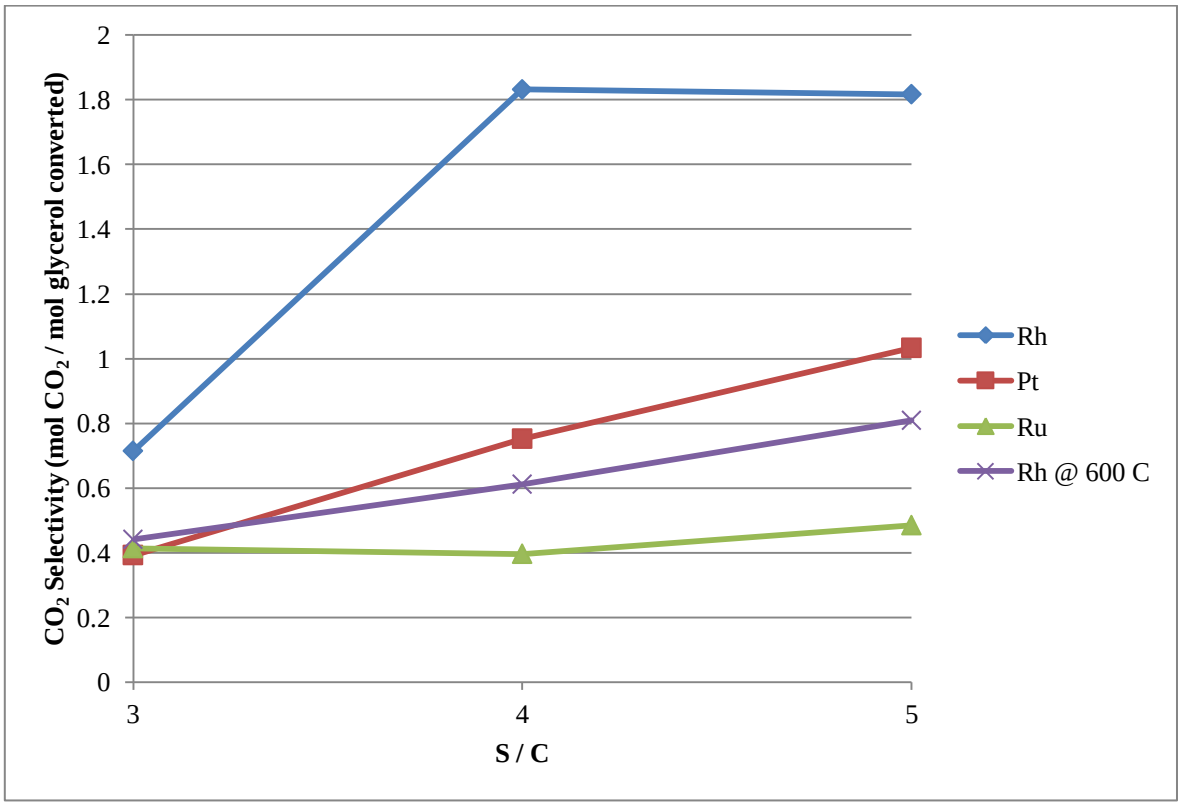

Figure 4.11. CO_2 Selectivity vs Steam-to-Carbon Ratio.

CH_4 selectivities, presented in Figure 4.12, show different behavior over different catalysts as steam-to-carbon ratio changes at different temperatures. Ru catalyst at 500 °C

does not produce any CH_4 at any steam-to-carbon ratio investigated. Similarly, Pt catalyst gives a very low CH_4 selectivity of 0.01 at 500 °C when steam-to-carbon ratio is 5. At lower steam-to-carbon ratios, no CH_4 selectivity is observed in the experiments over Pt catalysts. Rh catalyst exhibits an increasing CH_4 selectivity with increasing steam-to-carbon ratio. At steam-to-carbon ratio equals 3, CH_4 selectivity is 0.15. As steam-to-carbon ratio increases to 4 and 5, CH_4 selectivity increases to 0.23 and 0.30, respectively. Same Rh catalyst, however, causes an opposite trend of CH_4 selectivity at 600 °C as steam-to-carbon ratio increases. CH_4 selectivity is at its maximum, 0.25, at 600 °C when steam-to-carbon ratio is 3. When steam-to-carbon ratio is 4, CH_4 selectivity slightly decreases to 0.25. It reaches 0.18 as steam-to-carbon ratio decreases to 5.

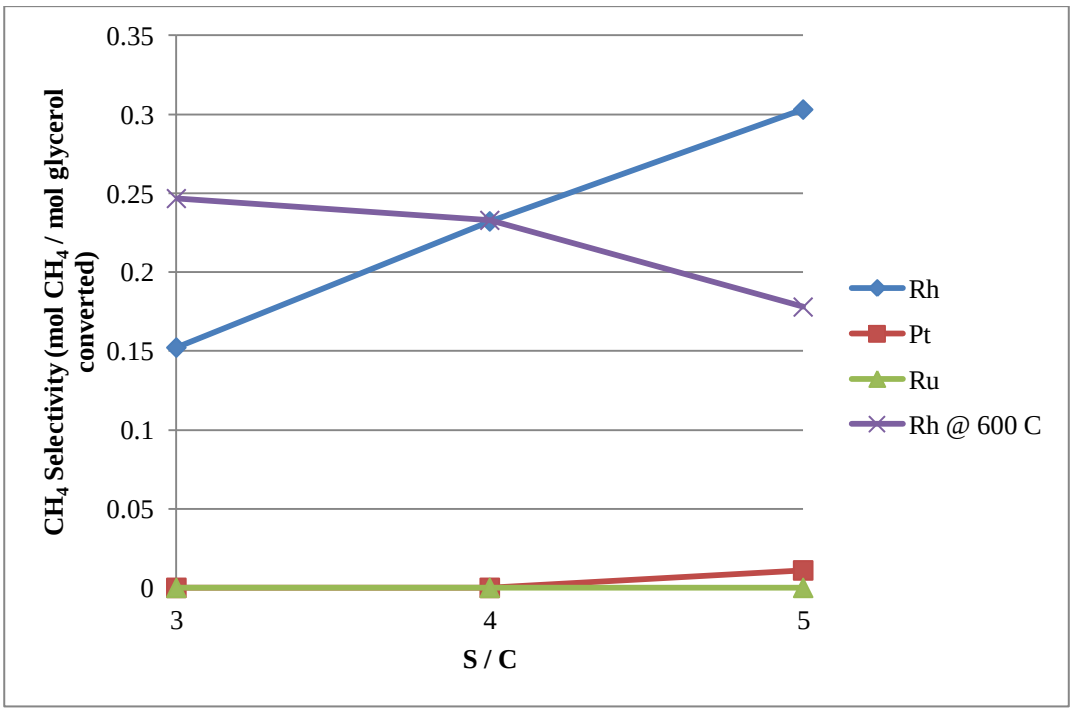

Figure 4.12. CH_4 Selectivity vs Steam-to-Carbon Ratio.

The reason of Rh catalyst giving higher CH_4 selectivity compared to those of Pt and Ru catalyst may be explained through their conversion levels obtained at 500 °C. There are several mechanisms that may lead to CH_4 production. One possible mechanism is the reaction of carbon (coke) with H_2. As the conversion obtained over Rh catalyst is 3 times the conversions obtained over Pt and Ru catalysts, the amount of H_2 in the reactor is much more in Rh catalyst case. As the H_2 amount increases, the probability of the contact of H_2

molecules and carbon deposited on the surface increases, which may result in CH_4 formation as Equation 2.4 suggests. Similarly, the amount of CO is also higher when conversion is high, which increases the chance of methanation reaction. CH_4 is also produced as a final product of side-reactions. Domination of side reactions may also affect CH_4 production. Increasing steam in the system reduces coke formation by significant amount in steam reforming reactions. As steam is increased, less coke is present, so the reaction of H_2 and carbon to give CH_4 is suppressed. This may explain the decreasing CH_4 selectivity trend with increasing steam-to-carbon ratio over Rh catalyst at 600 °C. Apparently, at 500 °C, another mechanism is more dominant, so that Rh catalyst gives more CH_4 selectivity with increasing steam-to-carbon ratio. It may be due to the H_2 selectivity, which sharply increases when steam-to-carbon ratio is 5. When the H_2 selectivity is high, the methanation reaction is positively affected, as the reaction equilibrium shifts to products' side.

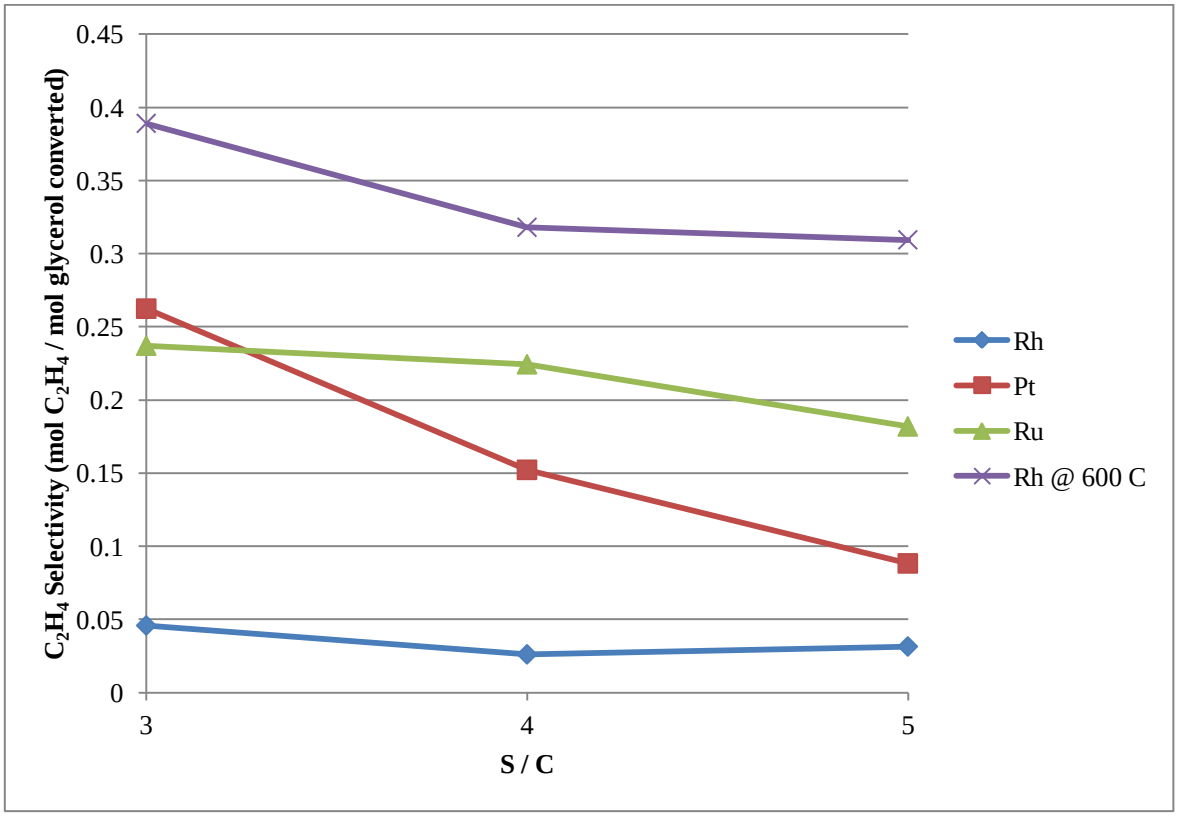

Figure 4.13. C_2H_4 Selectivity vs Steam-to-Carbon Ratio.

The effect of steam-to-carbon ratio on C_2H_4 selectivity is shown in Figure 4.13. Over Ru, Pt and Rh catalysts at 500 °C and over Rh catalyst at 600 °C, C_2H_4 selectivity slightly decreases with increasing steam-to-carbon ratio. Rh catalyst shows lower C_2H_4 selectivities compared with Ru and Pt catalysts at 500 °C. Same catalyst gives much higher C_2H_4 selectivity at 600 °C, still with a decreasing trend with increasing steam-to-carbon ratio. An increase in steam feed reduces coke formation. Ethylene is a byproduct that is capable of reacting further to produce carbon. A reaction environment with high steam content may favor the decomposition of glycerol to byproducts (like ethylene) less, which results in reduced coke formation.

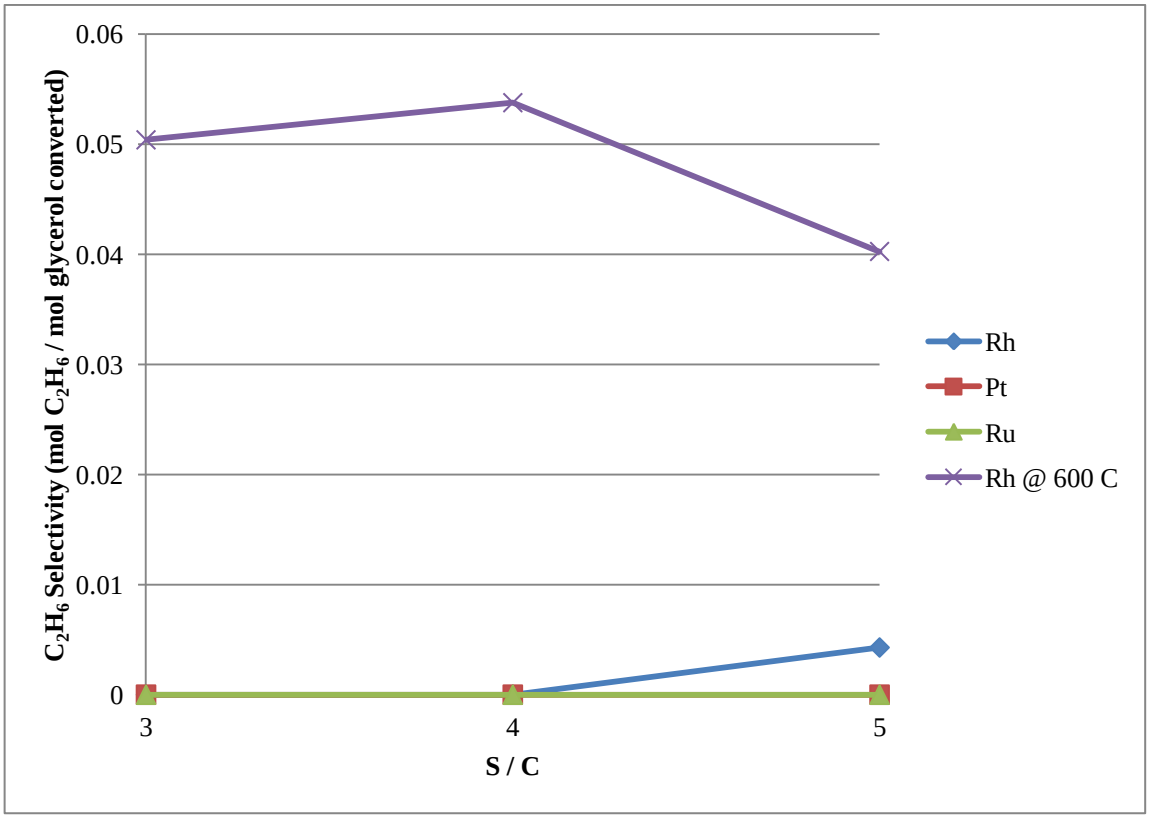

Figure 4.14. C_2H_6 Selectivity vs Steam-to-Carbon Ratio.

Rh, Pt and Ru catalysts shows no C_2H_6 production at 500 °C for steam-to-carbon ratios 3, 4 or 5. Same Rh catalyst gives higher C_2H_6 selectivities at 600 °C with a decreasing trend with steam-to-carbon ratio overall. Increasing steam content in the reactor may inhibit the byproducts (like C_2H_6), which have the potential to decompose into carbon.

Knowing that high steam-to-carbon ratios reduce coke formation, it perfectly adds up that the C_2H_6 selectivity is decreasing with increasing steam-to-carbon ratio.

4.3. Effect of Total Flow Rate

Effect of total flow rate on glycerol steam reforming reaction is investigated over 2 wt.% Rh/Al_2O_3 catalyst at 600 °C. Steam-to-carbon ratio is kept constant at 5. Three experiments are conducted, where total flow rates are set to 96 NmL min^{-1}, 128 NmL min^{-1} and 160 NmL min^{-1}. Outcomes of these experiments are given in Figure 4.15.

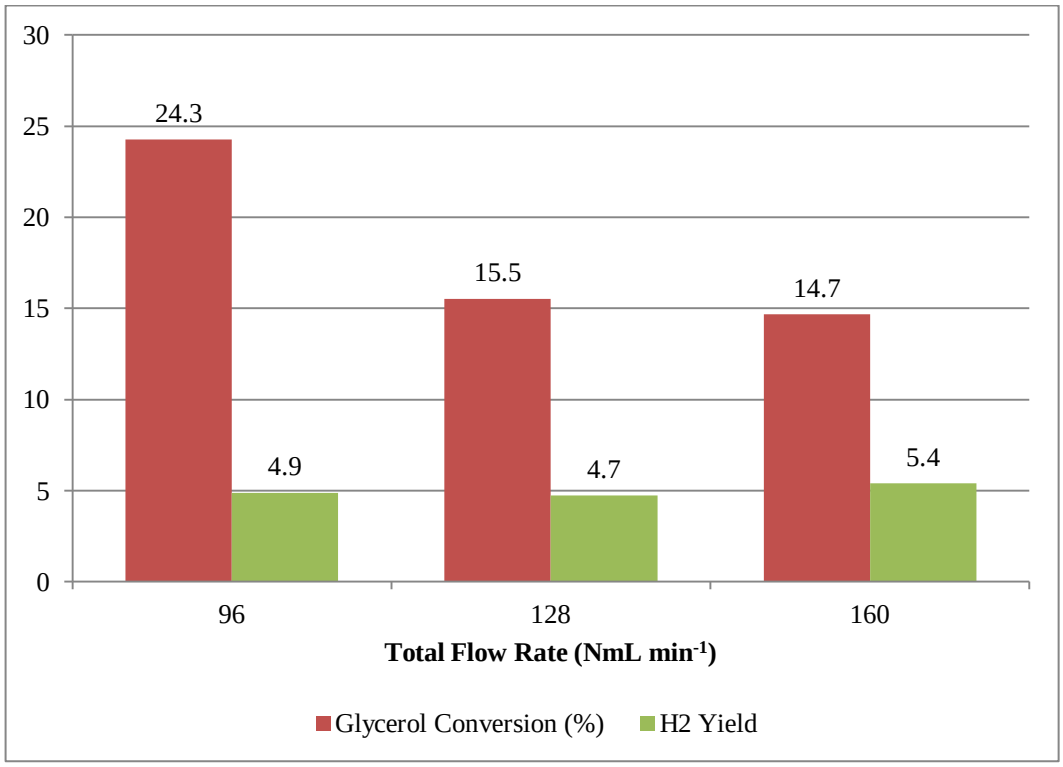

Figure 4.15. Glycerol Conversion and H_2 Selectivity vs Total Flow Rate.

As the total flow rate is increased from 96 NmL min^{-1} to 128 NmL min^{-1}, glycerol conversion decreased from 24.0% to 15.5%. As total flow rate is further increased to 160 NmL min^{-1}, conversion decreased only down to 14.7%. A decrease in glycerol conversion is expected as the reactants spend less time in the catalytic zone, the probability that they come into contact over active sites becomes less. It is concluded from these experiments,

that increasing the flow rate further does not create the same effect on glycerol conversion; conversion is much less affected when the total flow is further increased.

H_2 selectivity remains constant around 5 as flow rate is changed (Figure 4.15). H_2 selectivity first decreases very slightly from 4.9 to 4.7 and then it increases up to 5.4 with the total flow rate. As total flow rate is increased from 96 NmL min^{-1} to 128 NmL min^{-1}, conversion decreases significantly, but H_2 selectivity does not change. At high total flow rates, contact times are short, but high total flow rate is achieved through high reactant amount. These two adverse effects balance each other and H_2 selectivity stays constant.

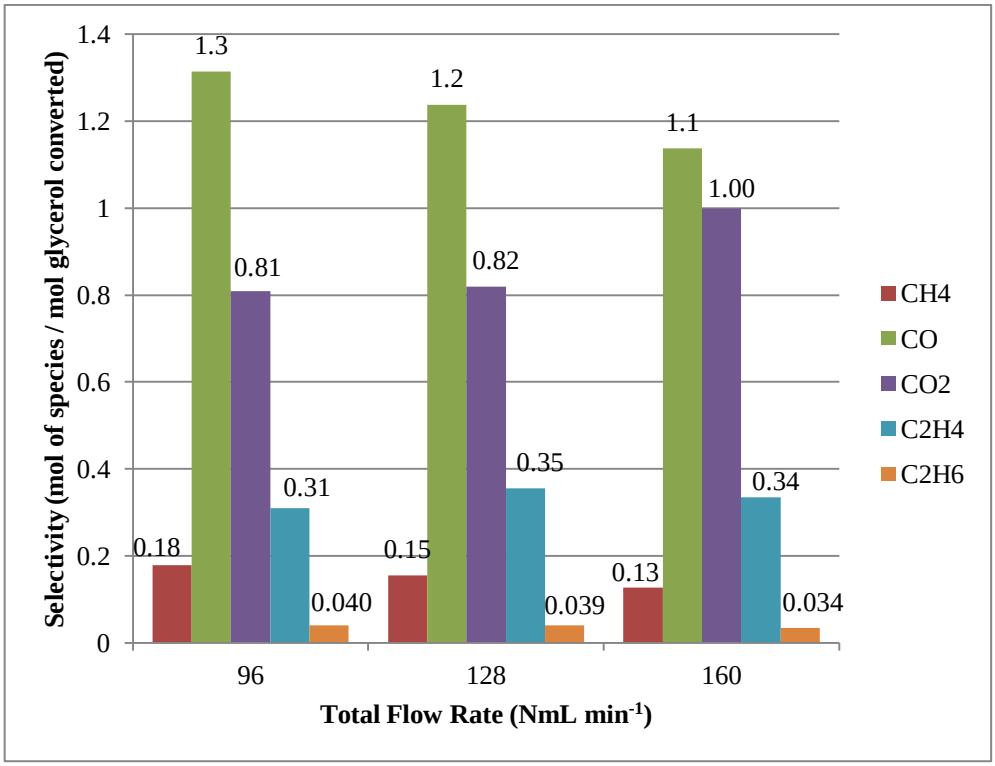

Figure 4.16. Selectivities of Gaseous Products vs Total Flow Rate.

Total flow does not affect H_2 selectivity too much, and neither any of those of other gaseous products (Figure 4.16). All of the species obey some increasing or decreasing trends with increasing flow rate, but the changes are minor. CO selectivity decreases from 1.3 to 1.1 as flow rate increases from 96 NmL min^{-1} to 160 NmL min^{-1}, which also cause increase in CO_2 selectivity from 0.81 to 1.00. When the increasing trends of H_2 and CO_2 selectivities and the decreasing trend of CO selectivity are considered, it can be speculated

that water gas shift reaction is having some increasing effect on product distribution. It seems that as the flow rate increases, water gas shift equilibrium shifts towards the products, leading to an increase in H_2 and CO_2 selectivity and a decrease in CO selectivity.

CH_4 and C_2H_6 selectivities decrease, but C_2H_4 selectivity increases with increasing total flow rate. The changes in the selectivities are, however, very minor. Although it is somewhat complicated to discuss the relationship between contact times and the reactions of intermediate products to final by products, it can be concluded that total flow rate does not have a significant effect on gaseous product selectivities. Total flow rate is only an important parameter for conversion.

4.4. Effect of Reactant Composition

Two experiments are compared with each other at 600 °C over 2 wt.% Rh/Al_2O_3 catalyst, keeping the steam-to-carbon ratio and total flow rate constant at 5 and 96 NmL min^{-1}, respectively, for observing the difference between a reaction involving 50% reactant gases and 50% inert, and 75% reactant gases and 25% inert. Outcomes of these experiments are shown in Figures 4.17 and 4.18.

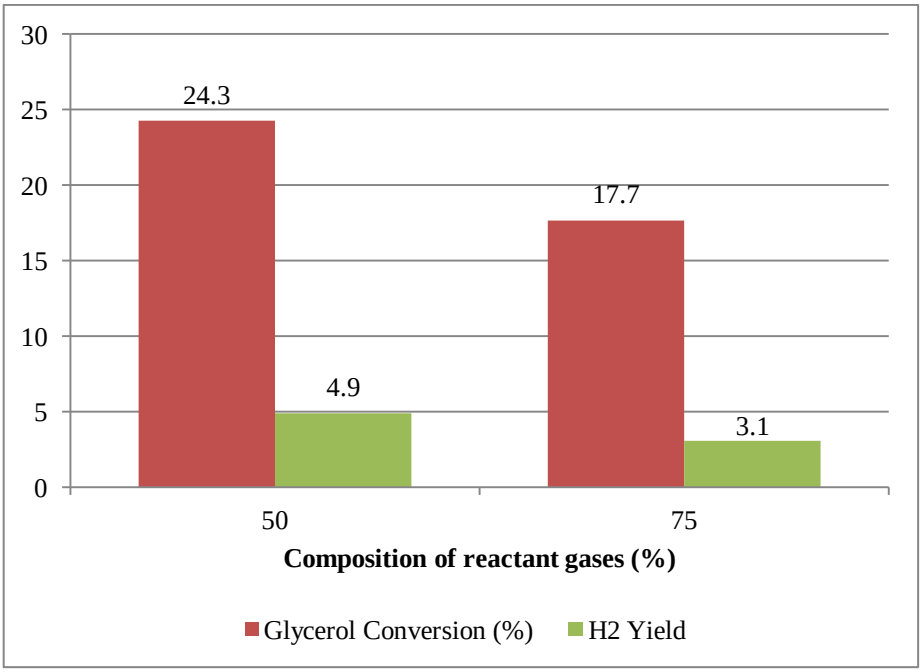

Figure 4.17. Glycerol Conversion and H_2 Selectivity vs Reactant Composition.

As the composition of reactants in the reactor is increased from 50% to 75%, a sharp decrease in glycerol conversion is observed. This is not expected, as normally an increase in the amount of reactants increase the chances of reaction occurring. One possible explanation is the fast rate of coke formation when the reactant gases are abundant. Supporting the same idea, another explanation may be the system configuration itself: Glycerol and water mixture approaches to the reactor in liquid phase. As the liquid reactants and the N_2 meet, N_2 sprays the liquid mixture into the upper zone of the furnace through a 1/16" tubing. Decreasing the amount of N_2 in the feed may have a negative effect on mixing in gas phase, because less amount of N_2 tries to spray a greater amount of liquid in to the furnace. If the N_2 flow is not enough to spray the reactants into the furnace, then an uneven mixing may take place, resulting in very low steam-to-carbon ratios at some spots, which may cause coke formation even before the reactants reach the catalytic zone.

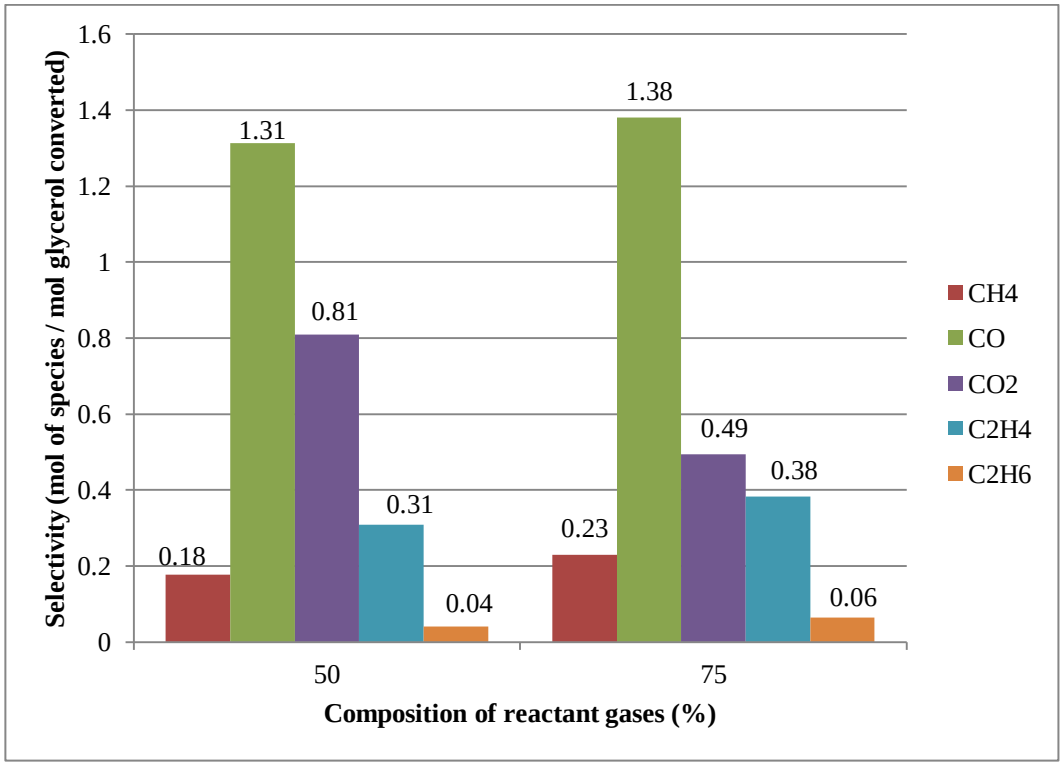

Figure 4.18. Selectivities of Gaseous Products vs Reactant Composition.

With two experiments in the hand, it is not very healthy to discuss about trends of product selectivities with changing reactant compositions. There is a slight increase in

CH_4, C_2H_4, C_2H_6 and CO selectivities as the composition of reactant gases increase from 50% to 75%. CO_2 selectivity decreases significantly. Decreases both in CO_2 and H_2 and increases in hydrocarbon selectivities suggest that glycerol decomposes into byproducts rather than steam reforming. A decrease in glycerol conversion and increases in selectivities of CH_4, C_2H_4 and C_2H_6 are strong indicators of coke formation when the reactant composition is increased.

4.5. Catalyst Characterization

Characterizations of reduced and spent Rh/Al_2O_3 catalysts are made by scanning electron microscopy (SEM) and energy dispersive X-ray spectroscopy (EDX) analyses. In order to understand the effect of temperature and steam-to-carbon ratio on catalyst surface, four spent catalyst samples are visually compared with each other and the reduced catalyst.

Four spent catalysts are exposed to 500 °C and 600 °C when steam-to-carbon ratio is 3 and 5. BSE images are created through the scattering electrons that are sent to the samples. The atoms scatter more electrons if they are larger, so larger atoms are seen as lighter spots, where smaller atoms are darker in color. In this case, bright spots are Rh atoms, gray regions are alumina and black regions are carbon. However, alumina is not a suitable material for SEM imaging and therefore the images have low resolutions. The images of the spent samples are indistinguishable. All of them have carbon particles and no agglomeration of Rh particles is observed. When the spent catalyst is compared with the reduced catalyst, the existence of carbon is easily realized.

EDX analysis is conducted to measure the amount (weight per cent) of Rh at Al_2O_3 surface. The targeted Rh weight percentage is 2 in this study. Nine random points are chosen and their Rh percentages on the surface determined by EDX. The average of nine points gives 1.96 wt.% Rh, which is very close to the targeted value.

Coke formation occurs in glycerol steam reforming at all temperatures and steam-to-carbon ratios selected in this study. However, the deposition of carbon on Rh/Al_2O_3 coated plate is not uniform. In the region where the reactants first come into contact with the plate, there is more carbon deposited (Figure 4.19). Moving on the plate towards the end, the

amount of carbon deposited decreases, clearly observed by looking at the catalyst (Figure 4.19). The case is also proven by EDX results. Unlike Rh, Pt and Ru coated spent samples show uniform carbon formation when looked at the plate with bare eyes.

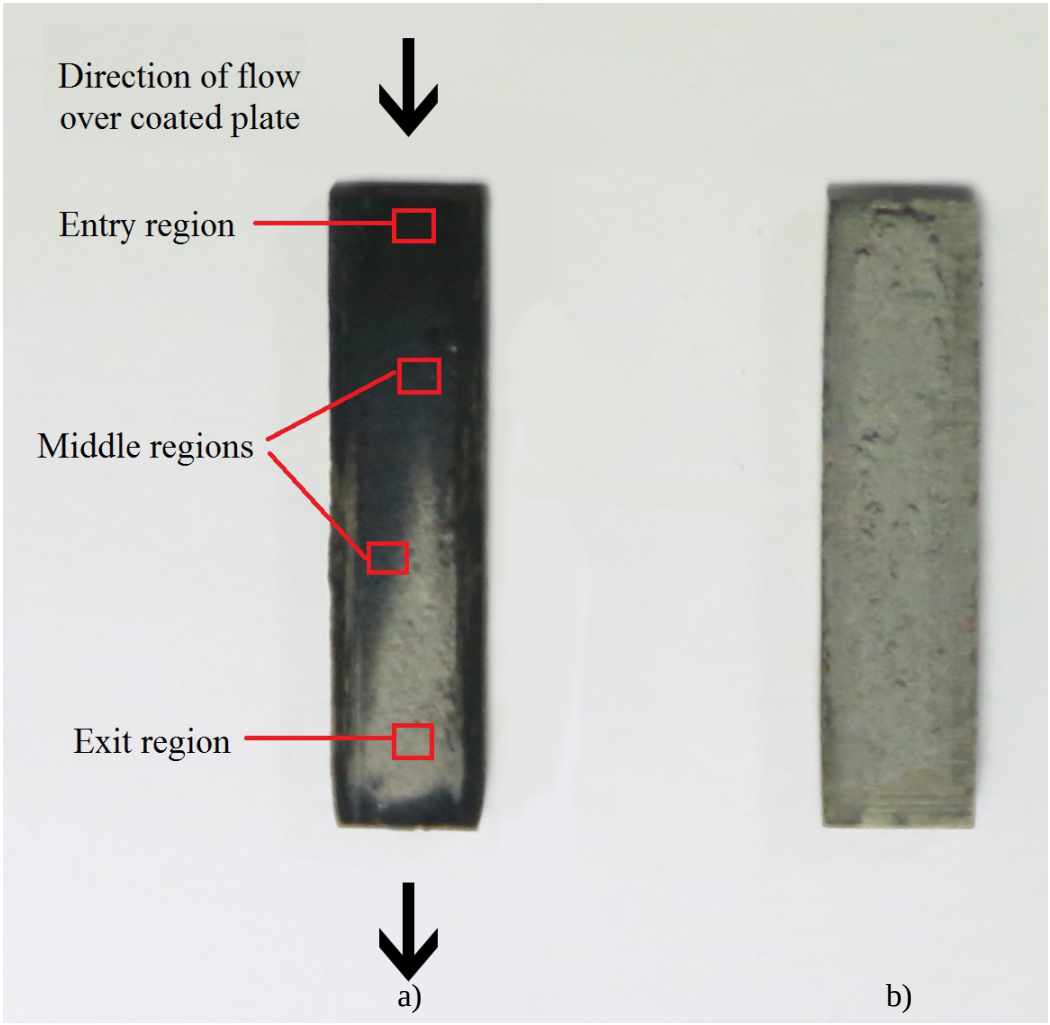

Figure 4.19. Catalyst-Coated Microchannel Plates a. Typical Spent Rh Catalyst (600 °C, S/C=3) b. Reduced Rh Catalyst.

Table 4.1. Surface composition of a typical spent Rh catalyst.

	Entry region	Middle region	Middle region	Exit region
C %	4.15	3.31	2.24	0.39
O %	33.00	31.49	36.53	32.63
Al %	61.10	63.35	59.65	64.67
Rh %	1.75	1.85	1.58	2.31

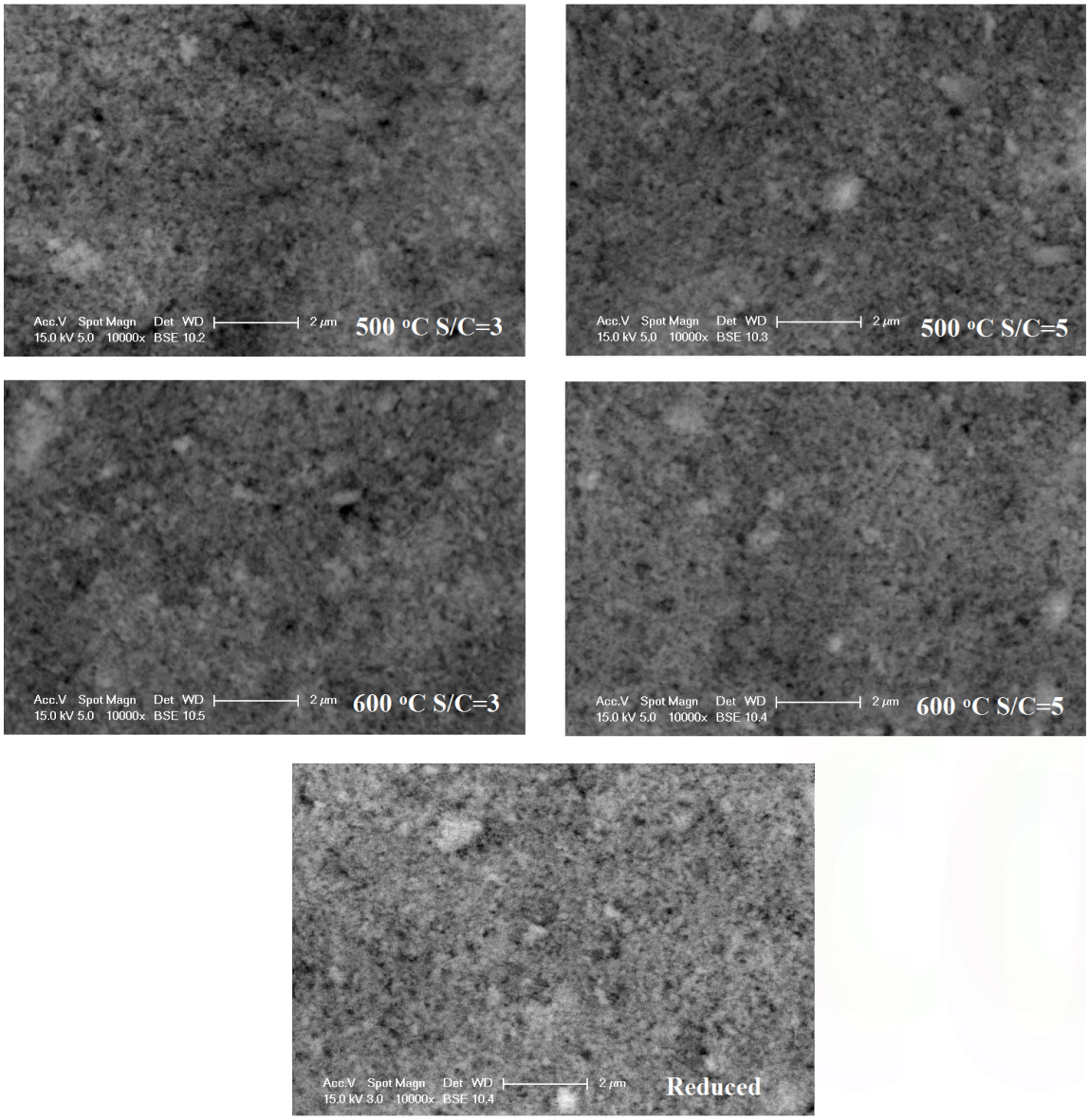

Figure 4.20. SEM Micro Images of Reduced and Spent Rh Catalysts.

In the entry region, the catalyst is exposed the reactants at most, so more carbon is formed on the entry region. Moving along the plate, the amount of carbon deposited is gradually reduced and in the exit region, carbon percentage reaches its minimum.

5. CONCLUSIONS AND RECOMMENDATIONS

5.1. Conclusions

In the study, glycerol steam reforming reaction is investigated over 2 wt.% Rh/Al_2O_3, 2 wt.% Pt/Al_2O_3 and 2 wt.% Ru/Al_2O_3 catalysts that are present in coated form in a microchannel reactor. The effect of temperature between 425 °C and 600 °C and steam-to-carbon ratio from 3 to 5 are analyzed over three different catalysts. In addition, the effects of total flow rate and reactant composition are experimented over 2 wt.% Rh/Al_2O_3. In each experiment, glycerol conversion and gaseous product selectivities are reported and compared with each other. Major conclusions of the parametric study of glycerol steam reforming are as follows:

- Rh/Al_2O_3 is the best catalyst in terms of glycerol conversion.
- Pt/Al_2O_3 at 475 °C and Rh/Al_2O_3 at 500 °C give maximum H_2 selectivities.
- Blank tests involving the components of the microchannel reactor (stainless steel housing and the FeCrAlY plate) show glycerol conversion levels comparable with those of Ru and Pt catalysts. This is probably due to high nickel content in the microchannel reactor components.
- Temperature is the key parameter to glycerol steam reforming. Glycerol conversion sharply increases over 500 °C. Product selectivities are also affected with temperature change. 500 °C is optimum for Rh/Al_2O_3 in terms of H_2 selectivity. As temperature increases further, H_2 selectivity decreases over all of the catalysts.
- Steam-to-carbon ratio is an important parameter as it directly affects the product distribution via the water gas shift reaction. Higher steam-to-carbon ratios lead to higher H_2 selectivities.
- An increase in total flow rate leads to a decrease in glycerol conversion, but no significant changes are observed on product selectivities.
- Increasing reactant composition in the system leads to a decrease in both glycerol conversion and H_2 selectivity.

- At high temperatures, CH_4, C_2H_4 and C_2H_6 selectivities increase sharply over all catalysts. Alumina is considered to boost side reactions such as dehydration, dehydrogenation and CO-removal due to its acidic character.
- Water gas shift reaction is important in glycerol steam reforming. In many cases, opposite behaviors of CO vs CO_2 and H_2 selectivities are observed, which points the dominance of water gas shift.
- Coke formation is inevitable in glycerol steam reforming. Over all three precious metal catalysts, even in blank tests, coke formation is observed. Amount of coke deposited is less on Rh-based catalysts.
- According to EDX results, targeted metal loading (2 wt.% Rh) is achieved in Rh catalyst. Spent Rh catalysts exhibit carbon formation, more carbon is deposited on entry region than exit region, EDX results show.

5.2. Recommendations

According to the results of this study, the recommendations to improve this research in the future are as follows:

- Liquid products and unreacted glycerol collected in cold traps can be analyzed using a GC/MS.
- Experiments can be repeated in a packed bed reactor, keeping the W/F ratio constant, to see the effect of reactor configuration.
- Alumina is known as a support that causes side reactions, so another support that is thermally stable, has a decent surface area and easy to apply on microplates can be tried instead of alumina.
- In this study, all precious metal catalysts are prepared to be 2 wt.%. Some experiments may be repeated over catalysts that have different metal percentages.
- Oxygen may be added as reactant to see if it reduces the coke formation and increases the catalyst life.
- Other non-precious active metals known for being good for steam reforming can be experimented in glycerol steam reforming.

APPENDIX A: CALIBRATION OF MASS FLOW CONTROLLERS

Calibration curves of the Bronkhorst mass flow controllers used in the experiments are given below.

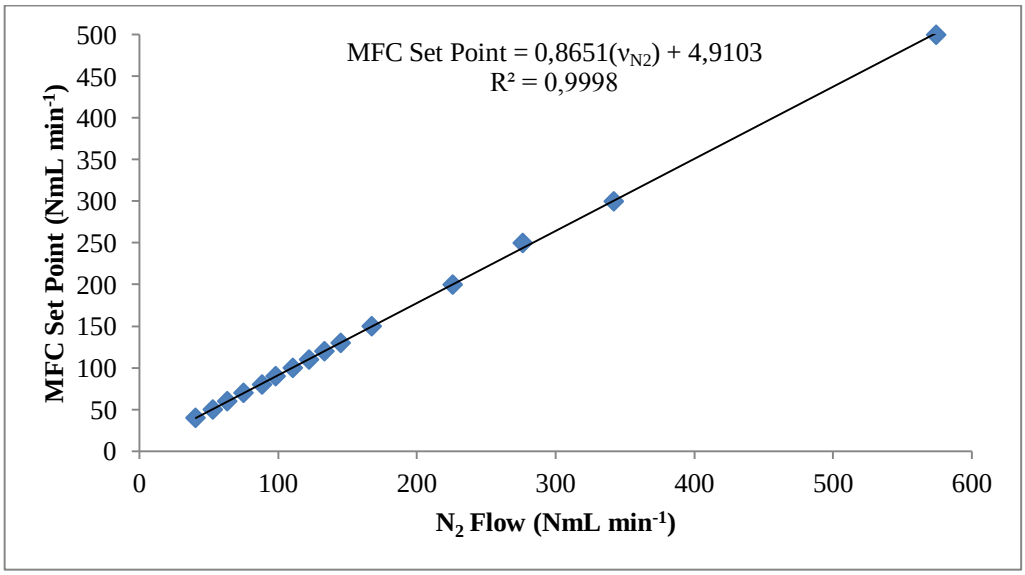

Figure A.1. Calibration Curve of the N_2 Mass Flow Controller.

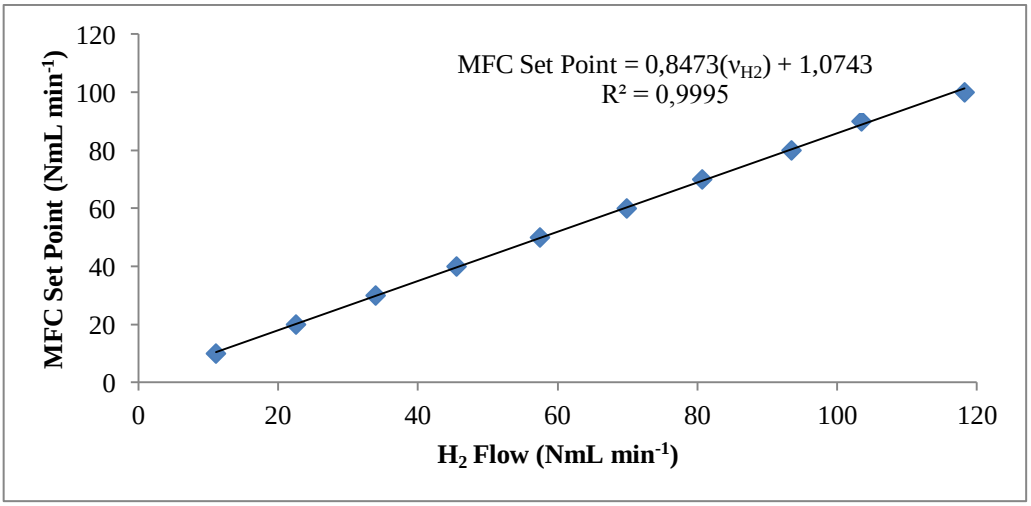

Figure A.2. Calibration Curve of the H_2 Mass Flow Controller.

APPENDIX B: CALIBRATION OF THE GAS CHROMATOGRAPHS

Calibration curves of gases analyzed at Shimadzu GC-2014 gas chromatograph equipped with Molecular Sieve 5A are given below.

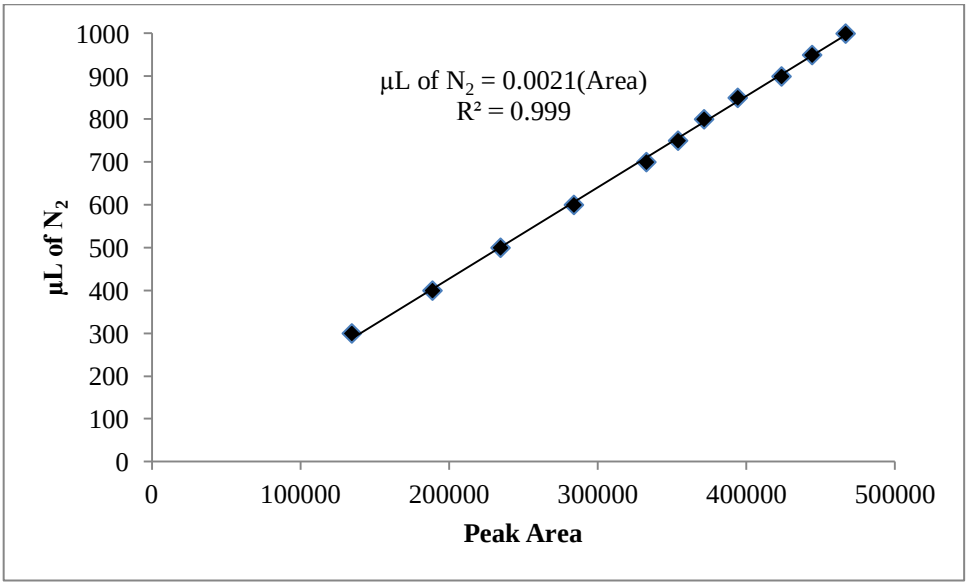

Figure B.1. Calibration Curve for N_2.

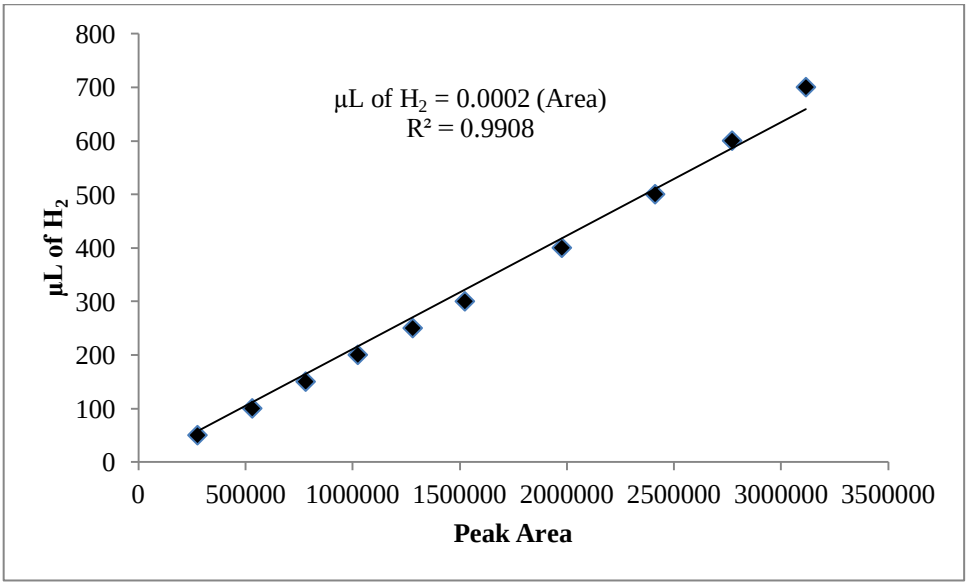

Figure B.2. Calibration Curve for H_2.

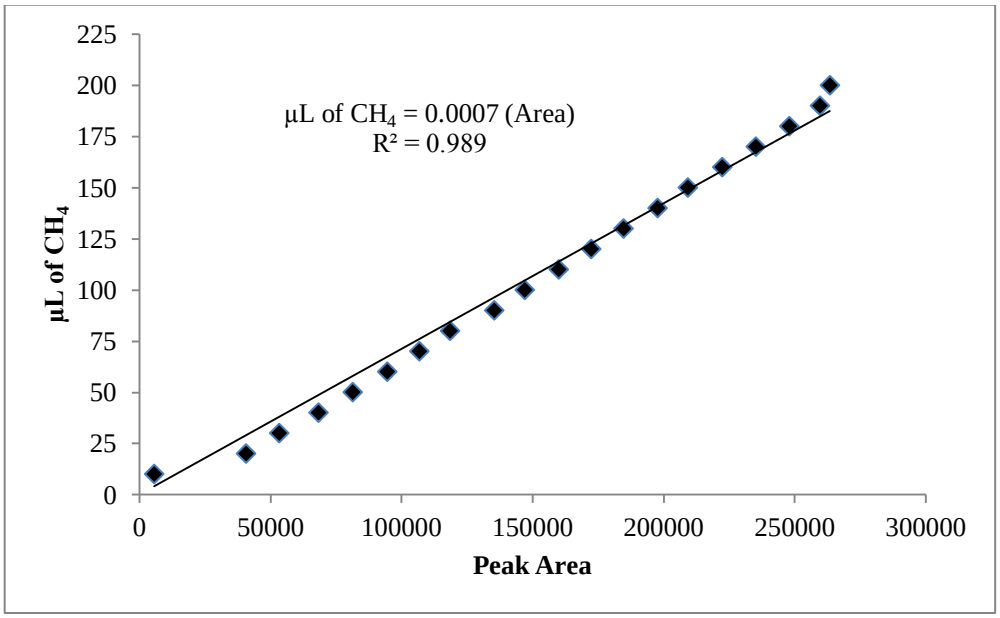

Figure B.3. Calibration Curve for CH_4.

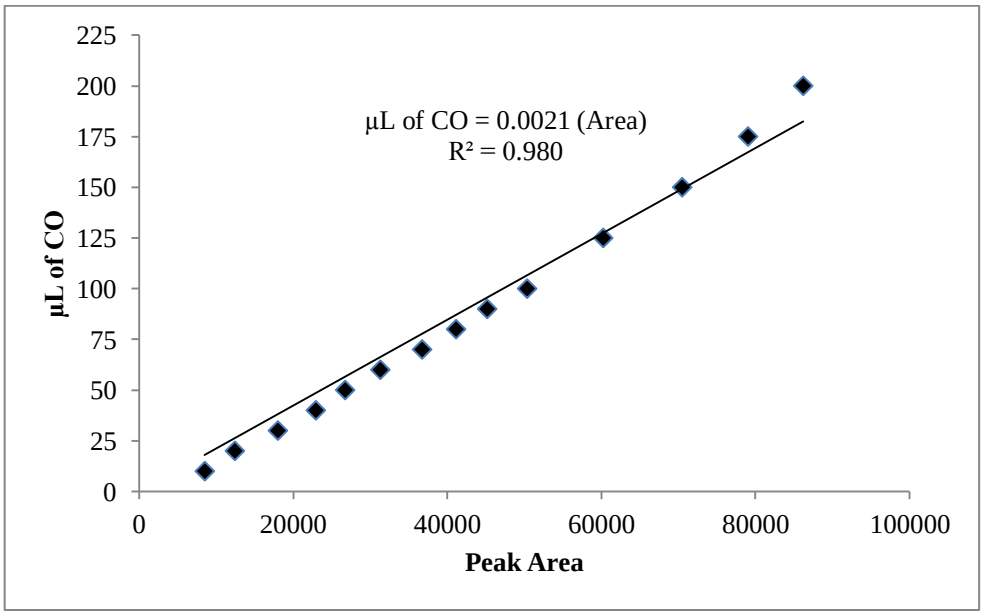

Figure B.4. Calibration Curve for CO.

Calibration curves of gases analyzed at Shimadzu GC-8A gas chromatograph equipped with Porapak Q are given below.

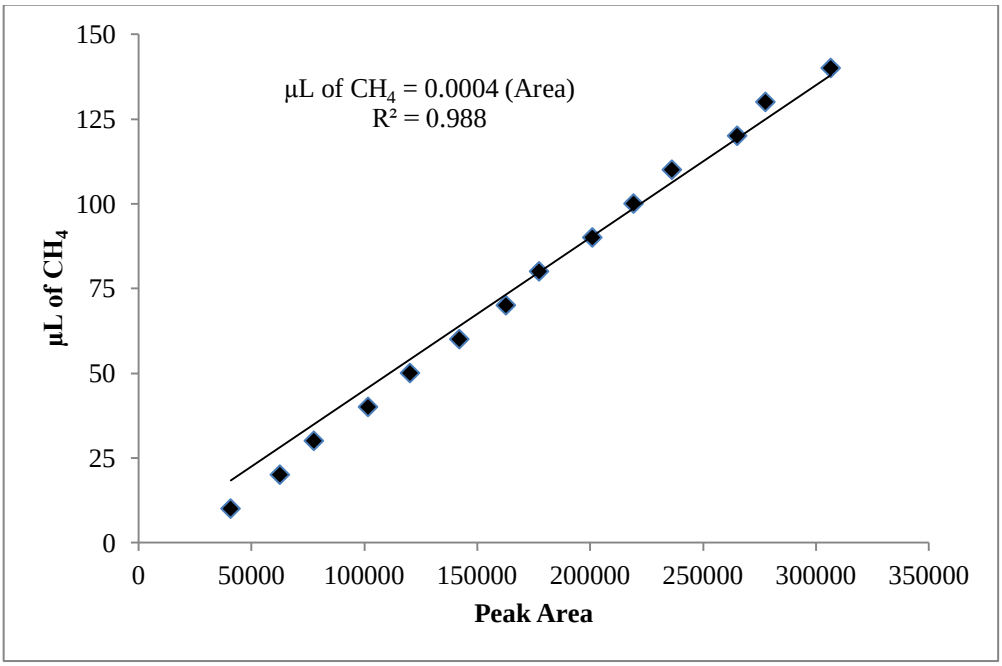

Figure B.5. Calibration Curve for CH_4.

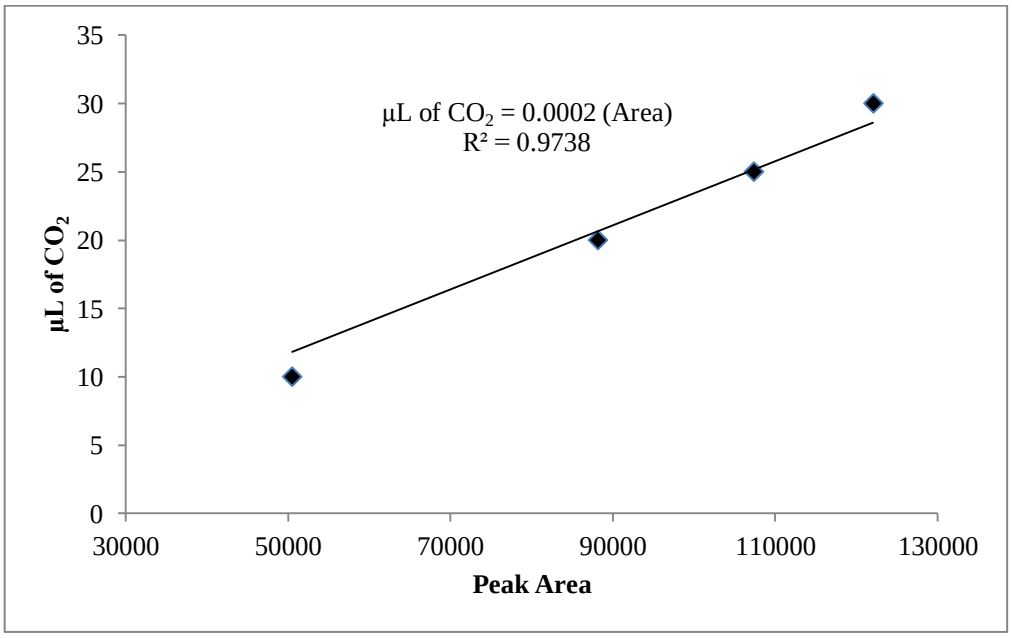

Figure B.6. Calibration Curve for CO_2.

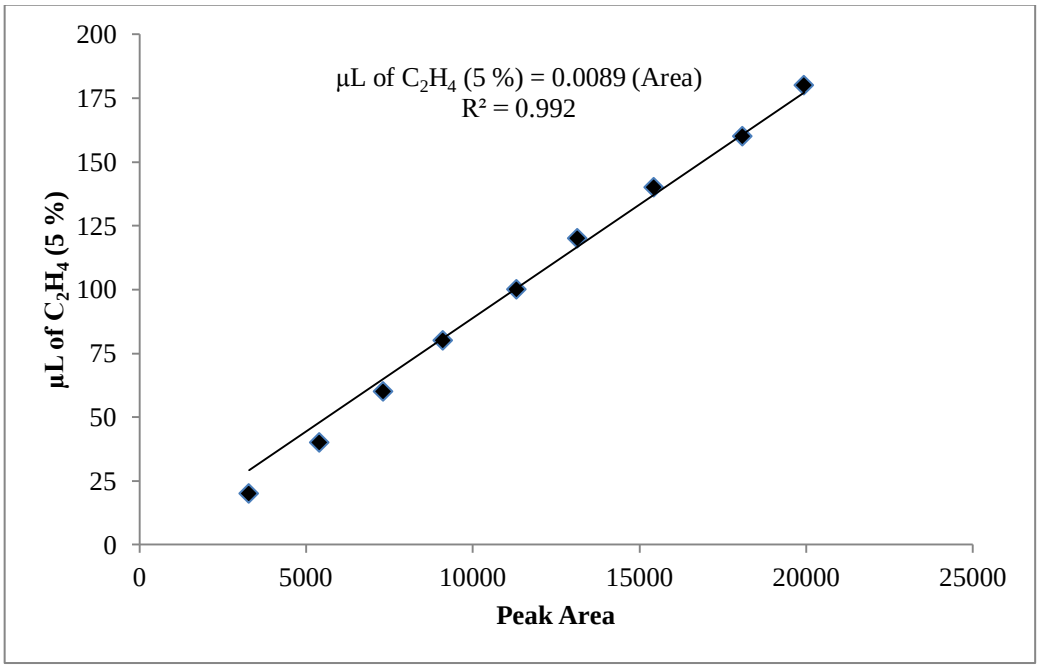

Figure B.7. Calibration Curve for C_2H_4.

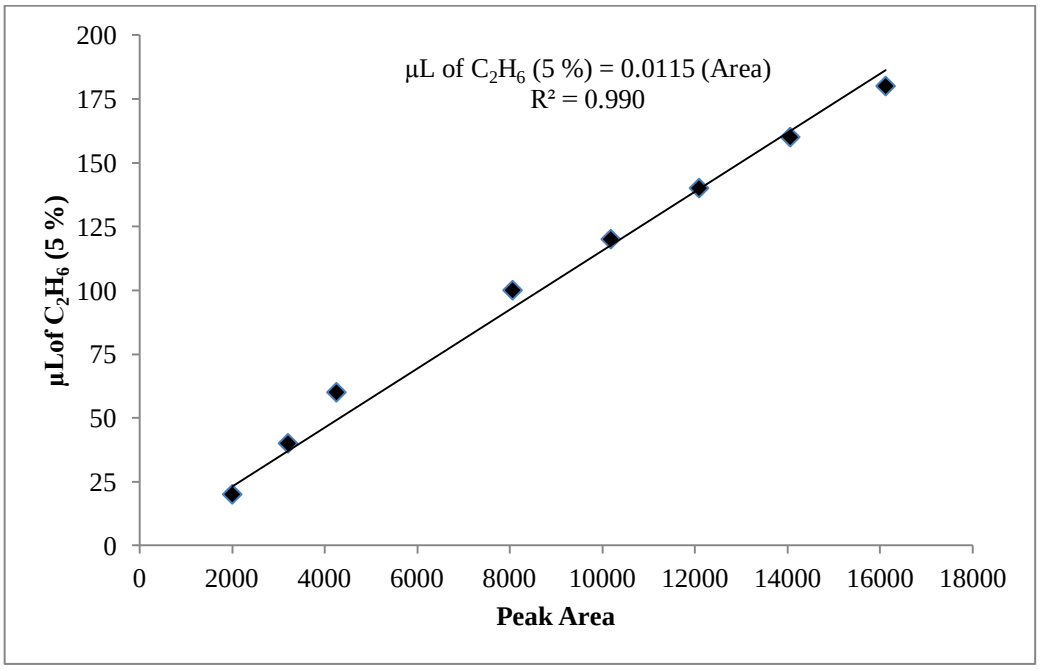

Figure B.8. Calibration Curve for C_2H_6.

REFERENCES

Avasthi, K. S., R. N. Reddy and S. Patel, 2013, "Challenges in the Production of Hydrogen from Glycerol - a Biodiesel Byproduct via Steam Reforming Process", *Procedia Engineering*, Vol. 51, pp. 423-429.

Avci, A. K., D. L. Trimm, A. E. Aksoylu and Z. I. Onsan, 2004, "Hydrogen Production by Steam Reforming of n-Butane over Supported Ni and Pt-Ni Catalysts", *Applied Catalysis A: General* , Vol. 258, pp. 235-240.

Chiodo, V., S. Freni, A. Galvagno, N. Mondello and F. Frusteri, 2010, "Catalytic Features of Rh and Ni Supported Catalysts in the Steam Reforming of Glycerol to Produce Hydrogen", *Applied Catalysis A: General*, Vol. 381, pp. 1-7.

Christoph, R., B. Schmidt, U. Steinberne, W. Dilla and R. Karinen, 2012, *Ullmann's Encyclopedia of Industrial Chemistry*, Wiley-VCH Verlag GmbH & Co. KGaA, Weinheim, Germany.

Dumesic, J. A., D. A. Simonetti and R. R. Soares, 2006, "Glycerol as a Source for Fuels and Chemicals by Low-Temperature Catalytic Processing", *Angewandte Chemie International Edition*, Vol. 118, pp. 4086-4089.

Doesburg, E. B. M., K. P. de Jong and J. H. C. van Hooff, 1999, *Catalysis: An Integrated Approach*, Elsevier, Amsterdam, Netherlands.

Ehrfeld, W., V. Hessel, and H. Löwe, 2000, *Microreactors: New Technology for Modern Chemistry***,** WILEY-VCH Verlag GmbH, Weinheim, Germany.

Fichtner, M., J. Mayer, D. Wolf and K. Schubert, 2001, "Microstructured Rhodium Catalysts for the Partial Oxidation of Methane to Syngas under Pressure", *Industrial & Engineering Chemistry Research*, Vol. 40, pp. 3475-3483.

Fornasiero, P., T. Montini, R. Singh, P. Das, B. Lorenzut, N. Bertero, P. Riello, A. Benedetti, G. Giambastiani, C. Bianchini, S. Zinoviev and S. Miertus, 2010, "Renewable H_2 from Glycerol Steam Reforming: Effect of La_2O_3 and CeO_2 Addition to Pt/Al_2O_3 catalysts", *ChemSusChem*, Vol. 3, pp. 619–628.

Goodfellow Group of Companies, 2014, *Fecralloy Material Information*, http://www.goodfellow.com/E/Fecralloy-Iron-Chromium.html, [Accessed October 2014].

Gupta, R. B., A. J. Byrd and K. K. Pant, 2008, "Hydrogen Production from Glycerol by Reforming in Supercritical Water over Ru/Al_2O_3 Catalyst", *Fuel*, Vol. 87, pp. 2956-2960.

Hasebe, S., 2004, "Design and Operation of Micro-Chemical Plants: Bridging the Gap between Nano, Micro and Macro Technologies", *Computers & Chemical Engineering*, Vol. 29, pp. 57-64.

Hessel, V. and G. Kolb, 2004, "Microstructured Reactors for Gas Phase Reactions" *Chemical Engineering Journal*, Vol. 98, pp. 1-38.

Iulianelli, A., P. K. Seelam, S. Liguori, T. Tongo, R. Keiski and V. Calabro, 2011, "Hydrogen Production for PEM Fuel Cell by Gas Phase Reforming of Glycerol as Byproduct of Bio-diesel: The Use of a Pd-Ag Membrane Reactor at Middle Reactor Temperature", *International Journal of Hydrogen Energy*, Vol. 36, pp. 3827-3834.

Karakaya, M., S. Keskin and A. K. Avcı, 2012, Parametric Study of Methane Steam Reforming to Syngas in a Catalytic Microchannel Reactor", *Applied Catalysis A: General*, Vol. 411-412, pp. 114-122.

Kiwi-Minsker, L., and A. Renken, 2005, "Microstructured Reactors for Catalytic Reactions", *Catalysis Today*, Vol. 110, pp. 2-14.

Lerou, J., A. Tonkovich, L. Silva, S. Perry, and J. McDaniel, 2010, "Microchannel Reactor Architecture Enables Greener Processes", *Chemical Engineering Science*, Vol. 65, pp. 380-385.

Lin, Y. C., 2013, "Catalytic Valorization of Glycerol to Hydrogen and Syngas", *International Journal of Hydrogen Energy*, Vol. 38, pp. 2678-2700.

Ma, L., 1995, *Hydrogen Production from Steam Reforming of Light Hydrocarbons in an Autothermic System*, Ph.D. Thesis, University of New South Wales.

Liu, S. K. and Y. C. Lin, 2012, "Autothermal Partial Oxidation of Glycerol to Syngas over Pt-, LaMnO3-, Pt/LaMnO3-coated Monoliths", *Industrial & Engineering Chemistry Research*, Vol. 51, pp. 16278-16287.

Nichio, N. N., F. Pompeo and G. Santori, 2010, "Hydrogen and/or Syngas from Steam Reforming of Glycerol, Study of Platinum Catalysts", *International Journal of Hydrogen Energy*, Vol. 35, pp. 8912-8920.

Sandmeyer Steel Company, 2014, *Specification Sheet: Alloy 310*, http://www.sandmeyersteel.com/310-310S.html, [Accessed October 2014].

Schmidt, L. D., P. J. Dauenhauer and J. R. Salge, 2006, "Renewable Hydrogen by Autothermal Steam Reforming of Volatile Carbohydrates", *Journal of Catalysis*, Vol. 244, pp. 238-247.

Schmidt, L. D., D. C. Rennard and J. S. Kruger, 2009, "Autothermal Catalytic Partial Oxidation of Glycerol to Syngas and to Nonequilibrium Products", *ChemSusChem*, Vol. 2, pp. 89- 98.

Schmidt, L. D., D. C. Rennard, J. S. Kruger and B. C. Micheal, 2010, "Longtime Behavior of the Catalytic Partial Oxidation of Glycerol in an Autothermal Reactor", *Industrial & Engineering Chemistry Research*, Vol. 49, pp. 8424-8432.

Slinn, M., K. Kendall, C. Mallon and J. Andrews, 2008, "Steam Reforming of Biodiesel By-product to Make Renewable Hydrogen", *Bioresource Technology*, Vol. 99, pp. 5851-5858.

Sundari, R., and P. D. Vaidya, 2012, "Reaction Kinetics of Glycerol Steam Reforming Using a Ru/Al_2O_3 Catalyst", *Energy & Fuels*, Vol. 26, pp. 4195-4204.

Sutar, P. N., P. D. Vaidya and A. E. Rodrigues, 2010, "Glycerol-Reforming Kinetics Using a Pt/C Catalyst", *Chemical Engineering Technology*, Vol. 33, pp. 1645-1649.

Suzuki, T., T. Hirai, T. Miyake and N. Ikenaga, 2005, "Production of Hydrogen by Steam Reforming of Glycerin on Ruthenium Catalyst", *Energy Fuels*, Vol. 19, pp. 1761-1762.

Veser, G. and J. Frauhammer, 2000, "Modeling Steady State and Ignition During Catalytic Methane Oxidation in a Monolith Reactor", *Chemical Engineering Science*, Vol. 55, pp. 2271-2286.

Watts, P. and C. Wiles, 2006, "Recent Advances in Synthetic Micro Reaction Technology", *Chemical Communications*, Vol. 5, pp. 443-467.